European air quality maps of ozone and PM_{10} for 2009 and their uncertainty analysis

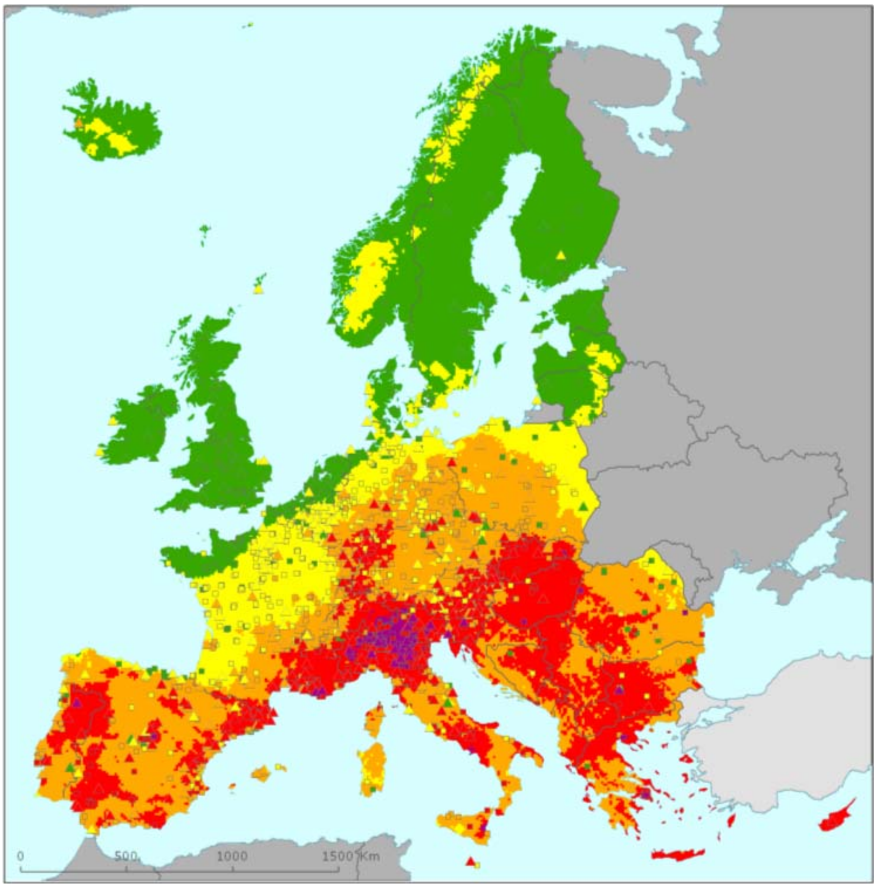

ETC/ACM Technical Paper 2011/11
December 2011

Peter de Smet, Jan Horálek, Pavel Kurfürst,
Markéta Schreiberová, Frank de Leeuw

European Topic Centre
on Air Pollution and
Climate Change Mitigation

The European Topic Centre on Air Pollution and Climate Change Mitigation (ETC/ACM)
is a consortium of European institutes under contract of the European Environment Agency
RIVM UBA-V ÖKO AEAT EMISIA CHMI NILU INERIS PBL CSIC

Front-page picture:
The ozone levels for the health indicators 26th highest daily maximum 8-hour value in µg.m^{-3} for both the rural and urban areas, combined into one final map for the year 2009. Its target value is 120 µg.m^{-3}. (Figure 5.1 of this paper).
Note the further decrease in the north and north-western European regions, versus an increase in specifically central and south-eastern Europe with ozone levels above the target value compared to those of 2008 (ETC/ACC Technical Paper 2010/11, cover picture). Furthermore, one may compare with the time series 2007—2005 (cover pictures of ETC/ACC Technical Paper 2009/9, 2008/8 and 2007/7, respectively).

Author affiliation:
Peter de Smet, Frank de Leeuw: National Institute for Public Health and the Environment (RIVM), Bilthoven, The Netherlands
Jan Horálek, Pavel Kurfürst, Markéta Schriberová: Czech Hydro meteorological Institute (CHMI), Praha, Czech Republic

Refer to this document as:
De Smet P, Horálek J, Kurfürst P, Schreiberová M, De Leeuw F (2012). European air quality maps of ozone and PM10 for 2009 and their uncertainty analysis. ETC/ACM Technical paper 2011/11 http://acm.eionet.europa.eu/reports/ETCACC_TP_2011_11_spatAQmaps_2009

DISCLAIMER

ETC/ACM Technical Paper 2011/11
European Topic Centre on Air and Climate Change Mitigation
PO Box 303
3720 AH Bilthoven
The Netherlands
Phone +31 30 2743562
Fax +31 30 2744433
Email etcacm@rivm.nl
Website http://acm.eionet.europa.eu/

Contents

1 Introduction

This paper provides an update of the European air quality concentrations, their exceedance probability and population exposure estimates for another consecutive year 2009. The analysis is based on interpolation of annual statistics of the 2009 observational data reported by EEA Member countries in 2010. The paper presents the mapping results and includes an uncertainty analysis of the interpolated maps, building upon the latest methodological developments of Horálek et al. (2007, 2008, 2010) and De Smet et al. (2009, 2010, 2011).

We consider in this paper again PM_{10} and ozone, as being the most relevant pollutants for annual updating. $PM_{2.5}$ is considered as a third important policy relevant pollutant and health impact indicator, but its mapping was still under development and has been dealt with in separate Technical Papers (De Leeuw and Horálek (2009); Denby et al. (2011a and 2011b); Gerharz et al. (2011) and Gräler et al. (2012)). With Denby et al. (2011b) this development reached a stage where we decided to include $PM_{2.5}$ in the annual mapping process for 2010 measurements and onwards.

The analysis of the year 2009 is similar to that of the year 2008. In this paper, we summarise the methodological and data updates applied to the 2009 data.

Next to annual indicator maps, we present in tables the population exposure to PM_{10} and ozone and the exposure of vegetation to ozone. These tables are prepared on the basis of 1x1 km grid resolution of both the combined final maps and the population density map.

For all the maps, we include a quantitative estimate of their interpolation uncertainty, using cross-validation parameters and scatter-plots. In addition, the paper contains the maps with probability estimates of limit/target value exceedances. For presentational purposes on European scale, we aggregated the 1x1 km grids into maps of a 10x10 km grid resolution, leading to considerably smaller figure file sizes.

Chapter 2 describes briefly the applied changes in methodology. Chapter 3 documents the updated input data. Chapters 4 and 5 present the calculations, the mapping, the exposure estimates and the uncertainty results for PM_{10} and ozone respectively. Chapter 6 summarizes the conclusions on exposure estimates and their interpolation uncertainties involved with the interpolated mapping of the air pollutant indicators.

2 Used methodology

2.1 Mapping method

Previous technical papers prepared by the ETC/ACC (Technical Papers 2010/10, 2009/16, 2009/9 2008/8, 2007/7, 2006/6, 2005/8 and 2005/7) discuss methodological developments and details on spatial interpolations and their uncertainties. No changes took place in the methodology in comparison with last year's report (De Smet et al., 2011). In this chapter a summary on the currently applied methods is given.

The mapping method used is the linear regression model followed by the kriging of its residuals (residual kriging). Interpolation is carried out according to the relation:

$$\hat{Z}(s_0) = c + a_1.X_1(s_0) + a_2.X_2(s_0) + ... + a_n.X_n(s_0) + \eta(s_0) \qquad (2.1)$$

where $\hat{Z}(s_0)$ is the estimated value of the air pollution indicator at the point s_o

$X_1(s_0), X_2(s_0), ..., X_n(s_0)$ are the n number of individual supplementary variables at the point s_o

$c, a_1, a_2, ..., a_n$ are the n selected parameters of the linear regression model calculated at the points of measurement,

$\eta(s_0)$ is the spatial interpolation of the residuals of the linear regression model at the points of measurement.

The spatial interpolation of residuals is carried out using ordinary kriging based on variogram estimates using a spherical function (with parameters: *nugget, sill, range*). For different pollutants and area types (rural, urban), different supplementary data are used, depending on their improvement to the fit of the regression.

For the PM_{10} indicators we apply prior to linear regression and interpolation a logarithmic transformation of concentrations on both the air quality measurements and the EMEP modelling output. For details, see De Smet et al. (2011). After interpolation we apply a back-transformation.

For the vegetation related indicators (AOT40 for crops and forests) we only construct rural maps based on rural background stations, based on the assumption that no vegetation is located in urban areas.

Health related indicator maps are constructed (linear regressions with kriging of its residuals) for the rural and urban areas separately on a 10x10 km grid resolution. The rural map is based on rural background stations and the urban map on urban and suburban background stations. Subsequent to that, the rural and urban maps are merged into one combined air quality indicator map using a European-wide population density grid on a 1 x 1 km grid resolution. For the 1 x 1 km grids with a population density less than a defined value of α_1, we select the rural map value, and for grids with a population density greater than a defined value α_2, we select the urban map value. For areas with population density within the interval (α_1, α_2) a weighting function of α_1 and α_2 is applied (for details and the setting of the parameters α_1 and α_2, see Horálek et al., 2008, 2007 and 2005). This applies in the grids where the estimated rural map value is lower in the case of PM_{10}, or higher in the case of ozone, than the estimated urban map value. In the minor areas with grid values for which this criterion does not hold, we apply a joint urban/rural map (created using all background stations regardless their type), as far as its value lies in between the rural and urban map value. For details, see De Smet et al. (2011).

Summarising, the separate rural, urban and joint urban/rural maps are constructed in a 10x10 km grid resolution; their merging takes place on basis of the 1 x 1 km population density grid resolution, resulting in a final combined pollutant indicator map on this 1x1 km grid resolution. This map is then used for population exposure estimates. At times we indicate the applied chain optimised combinations of spatial resolutions in the process of *interpolation* -> *merging* -> *exposure estimate* as the '10-1-1' (in km). For presentational purposes of European map pictures a spatially aggregation to

10x10 km^2 grids is sufficient. In all the calculations and map presentations, we use the EEA standard projection and datum defined as EEA ETRS89-LAEA5210.

For further details and discussion on subjects briefly addressed in this section, refer to De Smet et al. (2011), chapter 2.

2.2 Calculation of population and vegetation exposure

We base our population and vegetation exposure estimates on the interpolated concentration maps, population density data and land cover data.

2.2.1 Population exposure

Population exposure for individual countries and for Europe as a whole is calculated from the air quality maps and population density data, both at a 1x1 km resolution. For each concentration class, the total population per country as well as European-wide is determined. In addition, the population exposure per country and European-wide we expressed as the population-weighted concentration, i.e. the average concentration per inhabitant, according to

$$\hat{c} = \frac{\sum_{i=1}^{N} c_i p_i}{\sum_{i=1}^{N} p_i} \qquad (2.2)$$

where $\hat{c}$ is the population weighted average concentration in the country or in the whole Europe,
p_i is the population in the i^{th} grid cell,
c_i is the concentration in the i^{th} grid cell,
N is the number of grid cells in the country or in Europe as a whole.

2.2.2 Vegetation exposure

Vegetation exposure for individual countries and for Europe as a whole is calculated based on the air quality maps and land cover data, both in 2x2 km grid. For each concentration class, the total vegetation area per country as well as European-wide is determined.

2.3 Methods for uncertainty analysis

The uncertainty estimation of the European map is based on cross-validation. The cross-validation method computes the quality of the spatial interpolation for each measurement point from all available information except from the point in question, i.e. it withholds one data point and then makes a prediction at the spatial location of that point. This procedure is repeated for all measurement points of the available set. The predicted and measured values at these points are compared by drawing its scatter plot. With help of statistical indicators the quality of the predictions is demonstrated objectively – no suppositions have to be fulfilled. The advantage of the nature of this cross-validation technique is that it enables evaluating the quality of the predicted values at locations without measurements, as long as they are within the area covered by the measurements.

In addition, we make a simple comparison between the point measurements and interpolated values of the 10x10 km grid. The 10x10 km grid value is the averaged result of the interpolations for that 10x10 km area. The interpolated value within a grid cell will only approximate the predicted value(s) at the station(s) lying within that cell.

Another method to estimate uncertainties is based on geostatistical theory: together with the prediction, the prediction standard error is computed at all the grid cells, which represents in fact the interpolation uncertainty map (see Cressie, 1993 for a detailed discussion). Based on the concentration and the uncertainty map the exceedance probability map is created.

2.3.1 Cross-validation

The results of cross-validation are described by the statistical indicators and scatter plots. The main indicator used is root mean squared error (RMSE) and additional is the mean prediction error (MPE):

$$RMSE = \sqrt{\frac{1}{N}\sum_{i=1}^{N}(\hat{Z}(s_i) - Z(s_i))^2} \qquad (2.3)$$

$$MPE = \frac{1}{N}\sum_{i=1}^{N}(\hat{Z}(s_i) - Z(s_i)) \qquad (2.4)$$

where $Z(s_i)$ is the measured concentration at the i^{th} point, $i = 1, ..., N$,

$\hat{Z}(s_i)$ is the estimated concentration at the i^{th} point using other information, without the measured concentration at the i^{th} point,

N is the number of the measuring points.

RMSE should be as small as possible, MPE should be as close to zero as possible.

2.3.2 Comparison of the point measured and interpolated grid values

The comparison of measured and predicted grid values is described by the linear regression equation and its parameter and statistics values. The comparison is executed separately for rural and urban maps.

2.3.3 Exceedance probability mapping

The maps with the probability of exceedance (PoE) of a specific threshold value (e.g. limit or target value) are constructed using the concentration and uncertainty maps:

$$PoE(x) = 1 - \Phi(\frac{LV - C_c(x)}{\delta_c(x)}) \qquad (2.5)$$

where $PoE(x)$ is the probability of limit/target value (*LV/TV*) exceedance in the grid cell x,

$\Phi( )$ is the cumulative distribution function of the normal distribution,

LV is the limit or target value of the relevant indicator,

$C_c(x)$ is the interpolated concentration in the grid cell x,

$\delta_c(x)$ is the standard error of the estimation in the grid cell x.

The standard error of the probability map of the combined (rural and urban) map is calculated from the standard errors of the separate rural and urban maps, see Horálek et al. (2008) and De Smet et al. (2011). The maps with the probability of threshold value exceedance (PoE) are constructed in 10x10 km grid resolution.

3 Input data

The types of input data in this paper is not different from that of De Smet et al. (2011). The air quality, meteorological and, where possible, the supplementary data has been updated. No further changes in selecting and processing the input data have been implemented. For readability of this paper, we reproduce here the list of the input data. The key data is the air quality measurements at the monitoring stations extracted from AirBase. The supplementary data cover the whole mapping domain and is converted into the EEA reference projection ETRS89-LAEA5210 on a 10x10 km grid resolution, except for the AOT40 maps for which the data were converted – like last year – into a 2x2 km grid resolution to allow accurate land cover exposure estimates to be used in the Core Set Indicator 005 of EEA.

3.1 Measured air quality data

Air quality station monitoring data from 2009 are extracted from the European monitoring database AirBase (Mol et al. 2011), supplemented by several rural EMEP stations not reported to AirBase. Only data from stations classified by AirBase and/or EMEP of the type *background* for the areas *rural*, *suburban* and *urban* are used. *Industrial* and *traffic* station types are not considered; they represent local scale concentration levels not applicable at the mapping resolution employed. The following components and their indicators are considered:

PM_{10} – annual average [μg.m^{-3}], year 2009
– 36th maximum daily average value [μg.m^{-3}], year 2009

Ozone – 26th highest daily maximum 8-hour average value [μg.m^{-3}], year 2009
– SOMO35 [μg.m^{-3}.day], year 2009
– AOT40 for crops [μg.m^{-3}.hour], year 2009
– AOT40 for forests [μg.m^{-3}.hour], year 2009

SOMO35 is the annual sum of maximum daily 8-hour concentrations above 70 μg.m^{-3} (i.e. 35 ppb). AOT40 is the sum of the differences between hourly concentrations greater than 80 μg.m^{-3} (i.e. 40 ppb) and 80 μg.m^{-3}, using only observations between 7:00 and 19:00 UTC, calculated over the three months from May to July (AOT40 for crops), respectively over the six months from April to September (AOT40 for forests). Note that the term *vegetation* as used in the ozone directive is not further defined. Comparing the definitions in the Mapping Manual (UNECE, 2004) and those in the ozone directive suggests that we have to interpret the term *vegetation* in the ozone directive as agricultural crops. The exposure of *agricultural crops* has been evaluated here on basis of the AOT40 for vegetation as defined in the ozone directive.

For the indicators relevant to human health (i.e. PM10, and for ozone the 26th highest daily maximum 8-hour average and SOMO35) data from *rural*, *urban* and *suburban* background stations are considered. For the indicators relevant to vegetation damage (both AOT40 parameters for ozone) only *rural* background stations are considered.

Only the stations with annual data coverage of at least 75 percent are used. We excluded the stations from French overseas areas (departments), Svalbard, Azores, Madeira and Canary Islands. These areas we excluded from the interpolation and mapping domain. To reach a more extended spatial coverage by measurement data we use, in addition to the AirBase data, two additional rural background PM_{10} stations from the EMEP database. Table 3.1 shows the number of the measurement stations selected for the individual pollutants and their respective indicators. Compared to 2008, the number of stations selected for 2009 increased for the PM_{10} health indicators by approximately 7 % for rural and 4 % for urban background stations, for the ozone health indicators with some 4 % for rural and 3% for urban background stations and for both AOT40 indicators approximately 3 %.

Table 3.1 Number of stations selected for the individual indicators and areas. For rural areas the rural background stations and for urban areas the urban and suburban background stations are used.

	PM10		ozone			
	annual average	36th daily maximum	26th highest daily max. 8h	SOMO35	AOT40 for crops	AOT40 for forests
rural	289	289	501	501	505	506
urban	1102	1102	988	1022		

3.2 Unified EMEP model output

The chemical dispersion model used here is the Unified EMEP model (revision rv3_8_1), i.e. the EMEP/MSC-W model v.2011-06 according to the newly implemented nomenclature in the EMEP Status Reports (Fagerli et al. 2011), which is a Eulerian model with a resolution of 50 x 50 km. This model provides information on a 50 km x 50 km scale, that we converted to the 10x10 km grid cells, see below.

Contrary to the previous years, we received the EMEP data (with exception of SOMO35) in the form of daily means for PM_{10} and hourly means for ozone. We aggregated these primary data according annex B of Mol et al. (2011) to the same set of parameters as we have them for the air quality observations:

PM_{10} – annual average [µg.m^{-3}], year 2009 (aggregated from daily values)
– 36th maximum daily average value [µg.m^{-3}], year 2009 (aggregated from daily values)

Ozone – 26th highest daily maximum 8-hour average value [µg.m^{-3}], year 2009 (aggregated from hourly values)
– SOMO35 [µg.m^{-3}.day], year 2009
– AOT40 for crops [µg.m^{-3}.hour], year 2009 (aggregated from hourly values)
– AOT40 for forests [µg.m^{-3}.hour], year 2009 (aggregated from hourly values)

Simpson et al. (2003, 2011) and http://www.emep.int/OpenSource/index.html (EMEP web site) describe the model in more detail. The model results are based on emissions for the relevant year (Mareckova et al. 2011) and driven by ECMWF meteorology. Fagerli et al. (2011) provides details on the EMEP modelling for 2009.

In the original format, a point at its centre represents each grid cell (in 50x50 km resolution). The data are imported into *ArcGIS* as a point shapefile, subsequently converted into a 200x200 m raster grid, and spatially aggregated into the reference EEA 10x10 km grid.

3.3 Altitude

We use the altitude data field (in meters) of GTOPO30 that covers the European continent, with an original grid resolution of 30 x 30 arcsec. This data we converted into a 200x200 m grid resolution. For details, see Horálek et al. (2007) and spatially aggregated it into the reference EEA 10x10 km grid.

3.4 Meteorological parameters

Actual meteorological surface layer parameters we extracted from the Meteorological Archival and Retrieval System (MARS) of the ECMWF (European Centre for Medium-range Weather Forecasts). Currently we use the ECMWF variables (details specified in Horálek et al. 2007, Section 4.5) as supplementary data in the regressions:

Wind speed – annual average [m.s^{-1}], year 2009
Surface solar radiation – annual average [MWs.m^{-2}], year 2009

3.5 Population density and population totals

Population density [inhbs.km^{-2}], census 2001, we based on JRC data for the majority of countries (JRC, 2009) – source: EEA, pop01clcv5.tif, official version 5, 24 Sep. 2009, resolution 100x100 m.

For countries (Andorra, Albania, Bosnia-Herzegovina, Iceland, Liechtenstein, FYR of Macedonia, Montenegro, Norway, Serbia, Switzerland and Turkey) and regions (Faroe Islands, Jersey, Guernsey, Man, and northern part of Cyprus) which are not included in this map we used population density data from an alternative source: ORNL LandScan Global Population Dataset (ORNL, 2008).

The ORNL data is reprojected and converted from its original WGS1984 30x30 arcsec grids into EEA's reference projection ETRS89-LAEA5210 on a 1x1 km grid resolution by EEA (eea_r_3035_1_km_landscan-eurmed_2008, EEA (2008)). Furthermore, we compared the data on the one hand with JRC data for countries covered by both data sources, and on the other hand with Eurostat national population for 2009 (Eurostat, 2011). Figure 3.1 presents this comparison between ORNL and JRC data based on the national population totals of the individual countries.

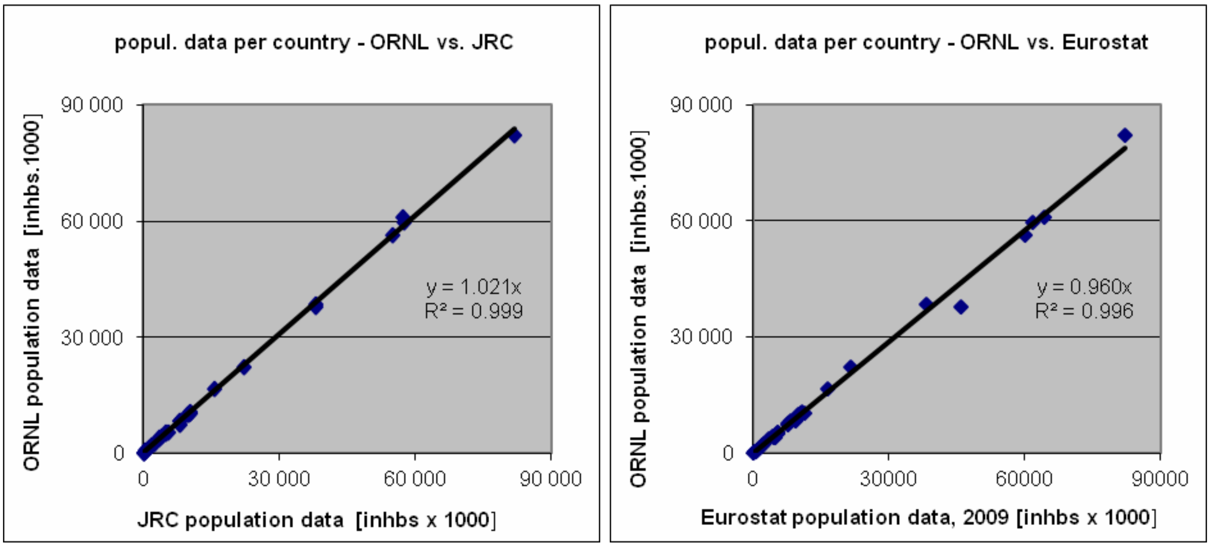

Figure 3.1 Correlation between ORNL (y-axis) and JRC (x-axis, left), respectively Eurostat 2009 revision (x-axis, right) national population totals.

The population density data was used to classify the spatial distribution of the type of areas (rural, urban or mixed population density) in Europe. We use it to select and weight the air quality value grid cell by grid cell. Furthermore, we use it to estimate the ultimate population health exposure and exceedance numbers per country and Europe as a whole, including involved uncertainties. These activities take place on a 1x1 km grid resolution as implementation of the recommendations of Horálek et al. (2010). For presentational purposed we construct maps on a 10x10 km grid resolution. To facilitate all this, we aggregated the JRC 100x100 m population density data into a 1x1 km grid, merged that with the ORNL dataset, and aggregated further into an additional 10x10 km grid map.

Population totals for individual countries presented in exposure tables in Section 4.2 and 5.2 are based on Eurostat national population data for 2009 (Eurostat, 2011). For countries (Andorra, Albania, Bosnia-Herzegovina, Monaco, San Marino, and Serbia) which are not included in the Eurostat database, the population totals are based on UN (2010) for 2010.

3.6 Land cover

The input data from CORINE Land Cover 2000 – grid 100 x 100 m, version 15 (08/2011) is used (CLC2000 – 100m, g100_00.zip; EEA, 2011). The countries missing in this database are Andorra and Turkey.

4 PM_{10} maps

This chapter presents the 2009 updates (for the interpolated map and exposures) of the two PM_{10} health indicators: annual average and 36th highest maximum daily average. The separate urban and rural concentration maps were calculated on a 10x10 km grid resolution and the subsequent combined concentration map was based on the 1x1 km gridded population density map. The population exposure tables are calculated on 1x1 km grid resolution. All maps are presented in a 10x10 km grid resolution. The standard EEA ETRS89-LAEA5210 was applied.

4.1 Annual average

4.1.1 Concentration map

Figure 4.1 presents the combined final map for the 2009 PM_{10} annual averages as the result of the interpolation and merging of the separate maps as described in detail in De Smet (2011) and Horálek et al. (2007). The red and purple areas and stations exceed the limit value (LV) of 40 $\mu g.m^{-3}$. Supplementary data in the regression used for rural areas consist of EMEP model output, altitude, wind speed and surface solar radiation, and for urban areas, it is EMEP model output only. (The relevant linear regression submodels have been identified earlier in Horálek et al. (2008) and De Smet et al. (2009, 2010, 2011) as P.Eawr and UP.E, respectively).

As one can observe in a few areas of the map, the high measurement values do not seem to influence the interpolation results despite their clustering. The main reason is that the map presented here is on a 10 x 10 km grid resolution. Whereas, the interpolation of the separate urban and rural map took place on a 1 x 1 km grid resolution and on basis of the 1 x 1 km population density map a 1 x 1 km combined final map has been composed, for presentational purposes a 10 x 10 km aggregation has been applied. This aggregation smoothes out the elevated values one would more likely be able to distinguish in the 1 x 1 km grid map, especially in the case of urban stations representing the urban areas. The exposure estimates of Table 4.1 are derived from the 1 x 1 km map. Another less prominent reason is the smoothing effect kriging has in general. The kriging would however in case of clustering not mask these elevations in the separate 1 x 1 km urban and rural map.

Table 4.1 presents the estimated parameters of the linear regression models (*c*, a_1, a_2,…) and of the residual kriging (*nugget, sill, range*), and includes the statistical indicators of both the regression and the kriging. The adjusted R^2 and standard error are indicators for the fit of the regression relation, where the adjusted R^2 should be as close to 1 as possible and the standard error should be as small as possible. The adjusted R^2 is 0.38 for the rural areas and 0.06 for urban areas. The R^2 values show a better fit of the regression than observed at year 2008 (0.29 and 0.00), 2006 (0.29 and 0.03) and 2005 (0.28 and 0.06), but slightly poorer fit than observed at the year 2007 (0.40 and 0.10) (De Smet et al. 2011, 2010 and 2009, Table 4.1; Horálek et al. 2008, Tables A.21 and A2.6). The low values for urban areas consistently over the years indicate that the fit of the regression in urban areas is poor (Horálek et al. 2007, 2008; De Smet et al. 2009, 2010, 2011). RMSE and MPE are the cross-validation indicators, showing the quality of the resulting map; the MPE indicates to what extent the estimation is un-biased. Section 4.1.3 deals with a more detailed analysis and compares with results of 2008, 2007, 2006 and 2005.

Table 4.1 Parameters of the linear regression models (Eq. 2.1) and of the ordinary kriging variograms (nugget, sill, range) - and their statistics - of PM_{10} indicator annual average for 2008 in the rural (left) and urban (right) areas as used for the combined final map, i.e. rural linear regression model P.Eawr (left), resp. urban UP.E (right) followed by interpolation of its regression residuals using ordinary kriging (OK, coded with 'a').

linear regr. model + OK on its residuals	rural areas (lnP.Eawr-a)	urban areas (lnUP.E-a)
	coeff.	coeff.
c (constant)	2.22	2.74
a1 (log. EMEP model 2008)	0.534	0.26
a2 (altitude GTOPO)	-0.00032	
a3 (wind speed 2007)	-0.157	
a4 (s. solar radiation 2008)	0.026	
adjusted R^2	**0.38**	**0.06**
standard error [μg.m^{-3}]	**0.30**	**0.35**
nugget	0.043	0.020
sill	0.080	0.055
range [km]	260	360
RMSE [μg.m^{-3}]	**4.62**	**6.67**
MPE [μg.m^{-3}]	**0.30**	**-0.04**

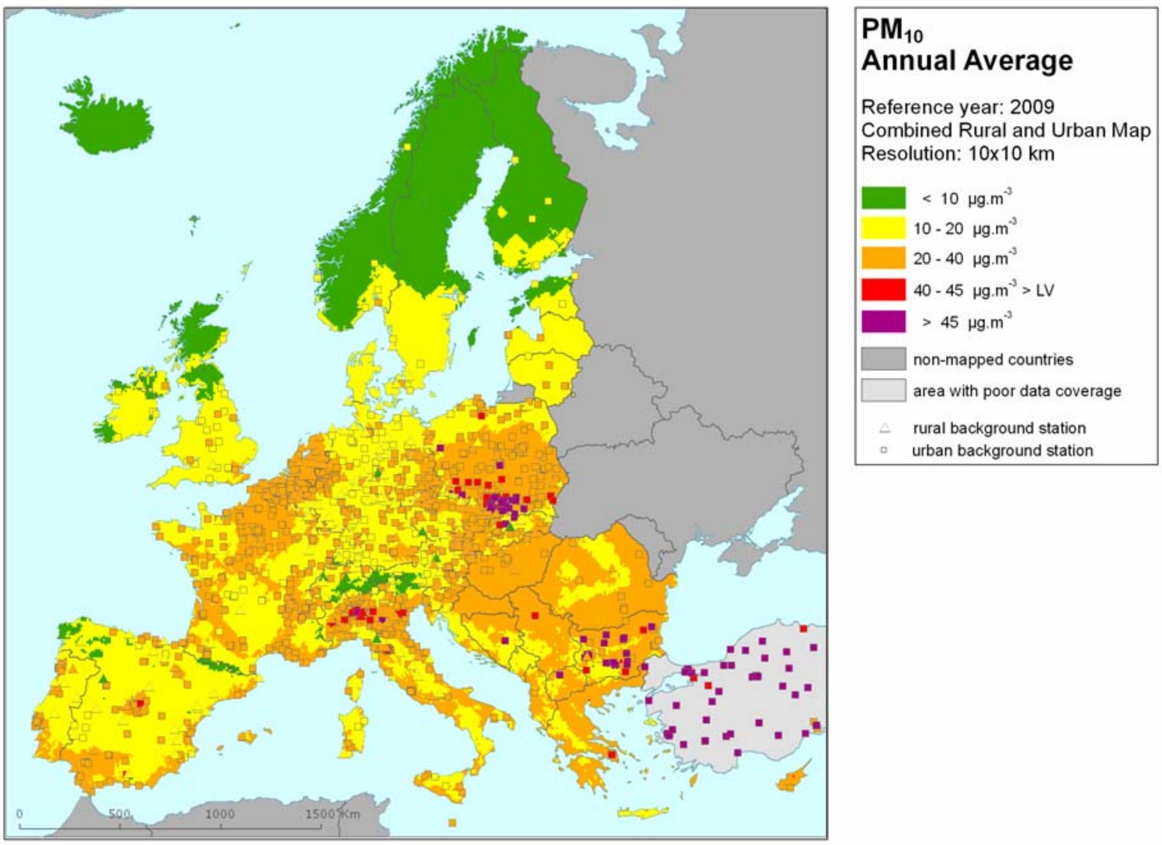

Figure 4.1 Combined rural and urban concentration map of PM_{10} – annual average, year 2009. Spatial interpolated concentration field and the measured values in the measuring points. Units: μg.m^{-3}.

4.1.2 Population exposure

Table 4.2 gives the population frequency distribution for a limited number of exposure classes calculated on a 1x1 km grid resolution, as well as the population-weighted concentration (i.e. the average concentration per inhabitant) for individual countries and for Europe as a whole according to Equation 2.2 of De Smet et al. (2010).
The merging of the separate rural and urban map takes place on a 1x1 km grid of the population density map. The application of this high resolution, now for the second consecutive year, induces a shift in the distribution of population over the different exposure classes as well as in the population-weighted concentrations. This will perturb the comparison of the 2009 and 2008 distributions with those of earlier years. Nevertheless, we compared between years, since tendencies within and between countries and regions seem not to deviate significantly between the two latest years and their preceding years.

Almost 30 % of the European population has been exposed to annual average concentrations below 20 $\mu g.m^{-3}$, the WHO (World Health Organization) air quality guideline. De Leeuw and Ruyssenaars (2011) estimate that 80 – 90 % of the urban population is exposed to levels above the WHO guideline reference level, i.e. 10 – 20 % below the WHO reference level. This lower amount accounts for specifically the urban population in the larger cities of Europe only, which naturally represents areas where in general considerably higher PM10 concentrations occur throughout the year. The estimate of Table 4.2 accounts also for all European population, including the rural areas, the smaller cities and villages which are in general will be exposed to lower levels of PM10 throughout the year. This difference in population characteristics and area representation accounted for in both estimates does explain the difference in the estimates. Two-third (66 %) of the European population lived in 2009 in areas where the PM_{10} annual mean concentration is estimated to be between 20 and 40 $\mu g.m^{-3}$. About 6 % of the population lived in areas where the PM_{10} annual limit value is exceeded, with Albania, Bosnia-Herzegovina, Bulgaria, Cyprus, FYR of Macedonia, Montenegro and Serbia (incl. Kosovo) showing in 2009 a population weighted concentration and/or a median above the LV. However, as the next section discusses the current mapping methodology tends to underestimate high values. Therefore, the exceedance percentage will most likely be higher and cause exceedance at a few more countries, for example Greece.

The frequency distribution shows a large variability over Europe, with the same countries showing exposures above the limit value as in 2008; some with considerable increase, others with a decrease. Bulgaria, FYR of Macedonia and Serbia with more than one fifth above LV in 2007, and about two-third or more in 2008 do show in 2009 still more then half of its population exposed to levels above the LV (BG 52%, MK 74%, RS 55%). Romania reduced considerably from about one-fifth population exposure in exceedance in 2007 and 2008 to approximately 4% in 2009.

Several countries with hardly any or no exceedances in 2007 did show in 2008 elevated PM_{10} annual averages well above the limit value. For example, in Cyprus this continues with 87 % in 2008 and 73% in 2009, caused by the one and only station reported, and additionally with an annual average value being in 2008 and 2009 well above the limit value and representing most of the Cypriot population. In Greece, the 37 % of 2008 reduced to 23 % in 2009, influenced by the limited number of stations with elevated values at specifically urban stations. FYR of Macedonia (68 % in 2008 and 74% in 2009), Serbia (62 % in 2008 and 55% in 2009) and Montenegro (36 % in 2008 and 60% in 2009) had limited number of stations showing rather elevated PM_{10} annual averages in 2008 and 2009. The strong fluctuation between the two years may have its cause in this limited number of stations as well as inter-annual variability induced by different dispersion conditions. Poland is on the same level as in 2007 and 2008 with around 12 – 15 % and Italy displays a slight increase from less than 3 % in 2008 to some 9 % in 2009 in exposure above limit value.

Two countries without exeedances in 2008 do show exceedances in 2009: Bosnia–Herzegovina (55%) and Croatia (3%). Albania shows a steep increase from 7% in 2008 to 52 % in 2009, likely caused by the limited number of stations (two). Czech Republic and Slovakia both show a similar limited exceedance of 2 % in 2008 and 1-3 % in 2009. Spain is the only country with exceedance in 2008 (1%) and no exceedance in 2009.

In a number of countries in north and northwestern Europe, the LV of 40 μg.m^{-3} seems not to be exceeded in continuation of previous years. When comparing 2009 with 2008, 2007, 2006 and 2005 we see that the population exposed to the low levels, i.e. below 20 μg.m^{-3}, has decreased slightly to some 29 % compared to the 31 % in 2008 but that is still better than for the years 2006 with 20 % and 2007 and 2005 with 24 % . The tendency of reducing exposure of population living in areas with concentrations above the limit value, from 9 % in 2005, through 7.7 % in 2006 and 5.7 % in 2007, seemed not to prolong in 2008 with its 5.8 % and in 2009 with 6.0 %.

Table 4.2 Population exposure and population weighted concentration – PM$_{10}$, annual average, year 2009. Resolution: 1x1 km.

Country		**Population**	**2009 Percent [%]**					**Population weighted conc.**
			< LV			**> LV**		
			< 10	**10 - 20**	**20 - 40**	**40 - 45**	**> 45**	
		x 1000	**μg.m^{-3}**	**μg.m^{-3}**	**μg.m^{-3}**	**μg.m^{-3}**	**μg.m^{-3}**	**μg.m^{-3}**
Albania	AL	3 204	0	6.6	41.3	46.1	6.0	35.3
Andorra	AD	85	10.2	89.8	0	0	0	17.7
Austria	AT	8 355	0.6	31.3	68.1	0	0	21.6
Belgium	BE	10 753	0	2.7	97.3	0	0	26.5
Bosnia & Herzegovina	BA	3 760	0	9.8	38.7	17.7	33.8	37.2
Bulgaria	BG	7 607	0.0	3.4	42.7	8.5	45.4	39.8
Croatia	HR	4 435	0.0	5.4	91.5	3.0	0	29.0
Cyprus	CY	797	0	0.1	26.8	24.0	49.1	41.0
Czech Republic	CZ	10 468	0	10.9	85.8	3.3	0	25.3
Denmark	DK	5 511	0.3	99.7	0.0	0	0	16.3
Estonia	EE	1 340	13.6	86.4	0	0	0	13.4
Finland	FI	5 326	21.0	79.0	0	0	0	11.7
France	FR	64 369	0.0	14.7	85.3	0	0	24.0
Germany	DE	82 002	0.0	36.9	63.1	0	0	20.7
Greece	GR	11 260	0.0	3.6	73.1	6.4	16.9	35.3
Hungary	HU	10 031	0.0	0.2	99.8	0	0	27.6
Iceland	IS	319	87.3	12.7	0	0	0	9.0
Ireland	IE	4 450	8.5	91.5	0	0	0	12.8
Italy	IT	60 045	0.1	7.6	83.5	8.8	0	28.7
Latvia	LV	2 261	0.1	40.8	59.2	0	0	18.8
Liechtenstein	LI	36	0	100.0	0	0	0	18.3
Lithuania	LT	3 350	0	47.5	52.5	0	0	19.0
Luxembourg	LU	494	0	23.5	76.5	0	0	21.0
Macedonia, FYROM of	MK	2 049	0	5.3	20.2	7.7	66.8	45.4
Malta	MT	414	0	0	100.0	0	0	27.2
Monaco	MC	35	0	0	100.0	0	0	26.8
Montenegro	ME	630	0	22.2	16.6	57.4	3.7	35.0
Netherlands	NL	16 486	0	4.5	95.5	0	0	24.3
Norway	NO	4 799	21.1	78.1	0.8	0	0	14.1
Poland	PL	38 136	0	7.5	77.7	8.0	6.7	30.8
Portugal	PT	10 627	0.0	23.4	76.6	0	0	22.9
Romania	RO	21 499	0	2.9	93.1	3.5	0.5	28.9
San Marino	SM	32	0	4.6	95.4	0	0	26.0
Serbia (incl. Kosovo)	RS	9 856	0	3.1	41.4	23.4	32.2	39.5
Slovakia	SK	5 412	0	8.7	90.2	1.1	0.0	26.9
Slovenia	SI	2 032	0	6.8	93.2	0	0	25.2
Spain	ES	45 828	0.9	18.1	80.9	0	0	23.7
Sweden	SE	9 256	8.5	91.5	0	0	0	13.8
Switzerland	CH	7 702	0.6	25.2	74.2	0	0	21.0
United Kingdom	UK	61 595	1.7	80.8	17.4	0	0	18.4
Total		**536 647**	**1.0**	**27.5**	**65.6**	**3.1**	**2.9**	**24.6**
			28.5			**6.0**		

Note: Turkey is not included in the calculation due to lacking population density data.

Considering the average for the whole of Europe, the overall population-weighted annual mean PM_{10} concentration in 2009 was 24.6 µg.m^{-3}. This is slightly lower than previous years: 0.2 µg.m^{-3} lower than in 2008 (De Smet et al. 2011), 0.7 µg.m^{-3} lower than in 2007 (De Smet et al. 2010), 2.5 µg.m^{-3} lower than in 2006 (De Smet et al. 2009) and 1.7 µg.m^{-3} lower than in 2005 (Horálek et al. 2008). The slight further decrease of the population-weighted concentration in comparison with 2008, 2007 and 2006 s occurs mainly in EU countries with few to none limit value exceedances.

4.1.3 Uncertainties

Uncertainty estimated by cross-validation

Using RMSE as the most common indicator, the *absolute mean uncertainty* of the combined final map at areas 'in between' the station measurements can be expressed in µg.m^{-3}. Table 4.1 shows that the absolute mean uncertainty of the combined final map of PM_{10} annual average expressed by RMSE is 4.6 µg.m^{-3} for the rural areas and 6.7 µg.m^{-3} for the urban areas. That is – together with 2007 - the lowest absolute uncertainty for rural areas, but the highest for the urban areas of the years 2005 - 2009. Alternatively, this uncertainty one could express in relative terms by relating the absolute RMSE uncertainty to the mean air pollution indicator value for all stations. This *relative mean uncertainty* of the combined final map of PM_{10} annual average 23.9 % for rural areas and 23.0 % for urban areas. This is for rural areas about the same as in 2007, but the highest of all mapping years. The higher uncertainty levels for urban areas in 2009 and 2008, compared to the years 2007 – 2005, are caused specifically by addition of Turkish urban background stations reported only since 2008. Since 2008 these data have been used in the calculations (although the interpolation result for Turkey is not present in the map due to lacking population density data used in the spatial assignment of urban and rural air quality concentrations in the final map). These relative uncertainty values fulfil the data quality objectives for models as set in Annex I of the 2008 air quality daughter directive EC (2008). Table 6.4 summarises both the absolute and relative uncertainties over these past five years.

Figure 4.2 shows the cross-validation scatter plots, obtained according Section 2.3 of De Smet et al. (2010), for both the rural and urban areas. The R^2 indicates that for the rural areas about 54 % and for the urban areas about 73 % of the variability is attributable to the interpolation. Corresponding values of the map of 2005 (52 % and 71 %), 2006 (52 % and 69 %), 2007 (59 % and 66 %) and 2008 (48 % and 82 %), show that for 2009 the fit at both the rural and urban interpolations is slightly above the average of the earlier four years.

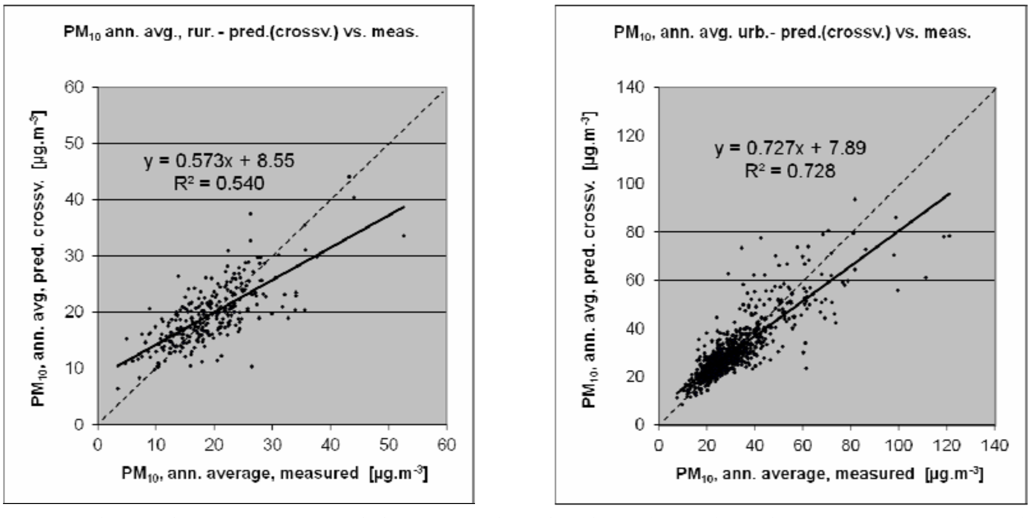

Figure 4.2 Correlation between cross-validation predicted values (y-axis) and measurements (x-axis) for the PM_{10} annual average for 2009 for rural (left) and urban (right) areas. R^2 and the slope a (from the linear regression equation $y = a{\cdot}x + c$) should be as close 1 as possible, the intercept c should be as close 0 as possible

The scatter plots indicate that in areas with high concentrations the interpolation methods tend to underestimate the levels. For example, in rural areas an observed value of 40 µg.m^{-3} is estimated in the interpolations about 30 µg.m^{-3}, about 25 % too low. This underestimation at high values is natural to all spatial interpolations. It can be reduced by either using a higher number of the stations at improved spatial distribution, or introducing a closer regression by using other supplementary data.

Comparison of point measurement values with the predicted grid value

Additional to the above point observation - point prediction cross-validation, a simple comparison has been made between the point observation values and interpolated prediction values averaged in a 10x10 km grid for the separate rural and urban map. This point-grid comparison indicates to what extent the predicted value of a grid cell represents the corresponding measured values at stations located in that cell. The results of the point observation - point prediction cross-validation of figure 4.2 compared to those of the point-grid validation are summarised in Table 4.3. The table shows a better correlated relation between station measurements and the interpolated values of the corresponding grid cells (i.e. higher R^2, smaller intercept and slope closer to 1) at both rural and urban map areas than it does at the point cross-validation predictions. That is because the simple comparison between point measurements and the gridded interpolated values shows the uncertainty at the actual station locations (points), while the point observation – point prediction cross-validation simulates the behaviour of the interpolation at positions without actual measurements within the area covered by measurements. The uncertainty at measurement locations is caused partly by the smoothing effect of the interpolation and partly by the spatial averaging of the values in the 10x10 km grid cells. The level of the smoothing effect leading to underestimation at areas with high values is there smaller than it is in case no measurement is represented in such areas. For example, in urban areas the predicted interpolation gridded value will be about 57 µg.m^{-3} at the corresponding station point with the measured value of 65 µg.m^{-3}, i.e. an underestimation of about 12 %.

Table 4.3 Linear regression equation and coefficient of determination R^2 from the scatter plots of (i) the predicted point values based on cross-validation and (ii) the aggregated predictions into 10x10 km grid cells versus the measured point values for PM_{10} indicator annual average for rural and urban areas of 2009.

	rural areas		urban areas	
	equation	R^2	equation	R^2
i) cross-validation prediction (Fig 4.5)	y = 0.573x + 8.55	0.540	y = 0.727x + 7.89	0.728
ii) 10x10 km grid prediction	y = 0.712x + 14.23	0.715	y = 0.794x + 5.64	0.867

Probability of Limit Value exceedance map

Next to the point cross-validation analysis, we constructed the map with the probability of limit value exceedance. For this purpose, we aggregated the 1x1 km gridded combined final concentration map into a 10x10 km grid map. Then we derived with support of the 10x10 km uncertainty map and the limit value (40 µg.m^{-3}) the probability of exceedance (PoE) map on a 10x10 km grid resolution (Figure 4.3).

The map demonstrates areas with a probability of limit value exceedance above 75 % marked in red (*high* probability) and areas below 25 % in green (*low* probability). Red indicates areas for which exceedance may occur *very likely* due to either high concentrations close to or already above the LV accompanied with such uncertainty that exceedance is very likely, or areas with lower concentrations accompanied with high uncertainty levels reaching above the LV that excess is very likely. Vice versa, in the green areas it is *not likely* to have predicted concentrations and accompanying uncertainties at levels that do reach above the LV.

In the probability maps the areas with 25-50 %, resp. 50-75 % probability of LV exceedance are marked in yellow and orange. The yellow colour indicates the areas with the estimated concentrations below limit value, but for which there exist a *modest* probability of exceeding the limit. On the contrary, the orange areas have estimated concentrations above the limit value, but with a chance of non-exceedance caused by its accompanying uncertainty. Table 4.4 summarises the classes and terminology for probability (i.e. likelihood) that will be distinguished in this paper.

The patterns in the spatial distribution of the different PoE classes over Europe differ in 2009 not much from those of 2008. It shows some more elevated probability of exceedances (50-75 % and 75-100 %) at just some limited areas where in 2008 only modest PoE occurred. Nevertheless, these are still considerably smaller then the more elevated areas as mapped in 2007-2005. It involves the Po Valley in Italy at Milan and Turin, the region of South Poland – North-East Czech Republic with the industrial zone of Krakow, Katowice (PL) and Ostrava (CZ). In south-eastern Europe, where relative few measurement stations are located, only at some larger agglomerations with mostly high traffic density and heavy industry such elevated PoE do show up, such as in Bulgaria at Sofia and Plovdiv including its industrialised region South-East of that city. Again, it deals with levels somewhat higher than in 2008 but still smaller and lower than at those of 2007-2005. Furthermore, some moderate PoE occurs just at the largest agglomerations on Cyprus. In Greece, only Thessaloniki shows modest PoE. In the other parts of Europe, there exists just little likelihood of exceedance. Overall conclusion can be that the likelihood of exceedance in 2009 is slightly higher, but in a more restricted area compared to the levels of 2008.

Table 4.4 Probability mapping classes and terminology use in this paper.

Map class colour	Percentage probability of threshold exceedance	Degree of probability (/ likelihood) of exceedance	Likelihood of exceedance
Green	0 – 25	Low/ Little	Not likely
Yellow	25 – 50	Modest	Somewhat likely
Orange	50 – 75	Moderate	Rather Likely
Red	75 – 100	High / Large	Very likely

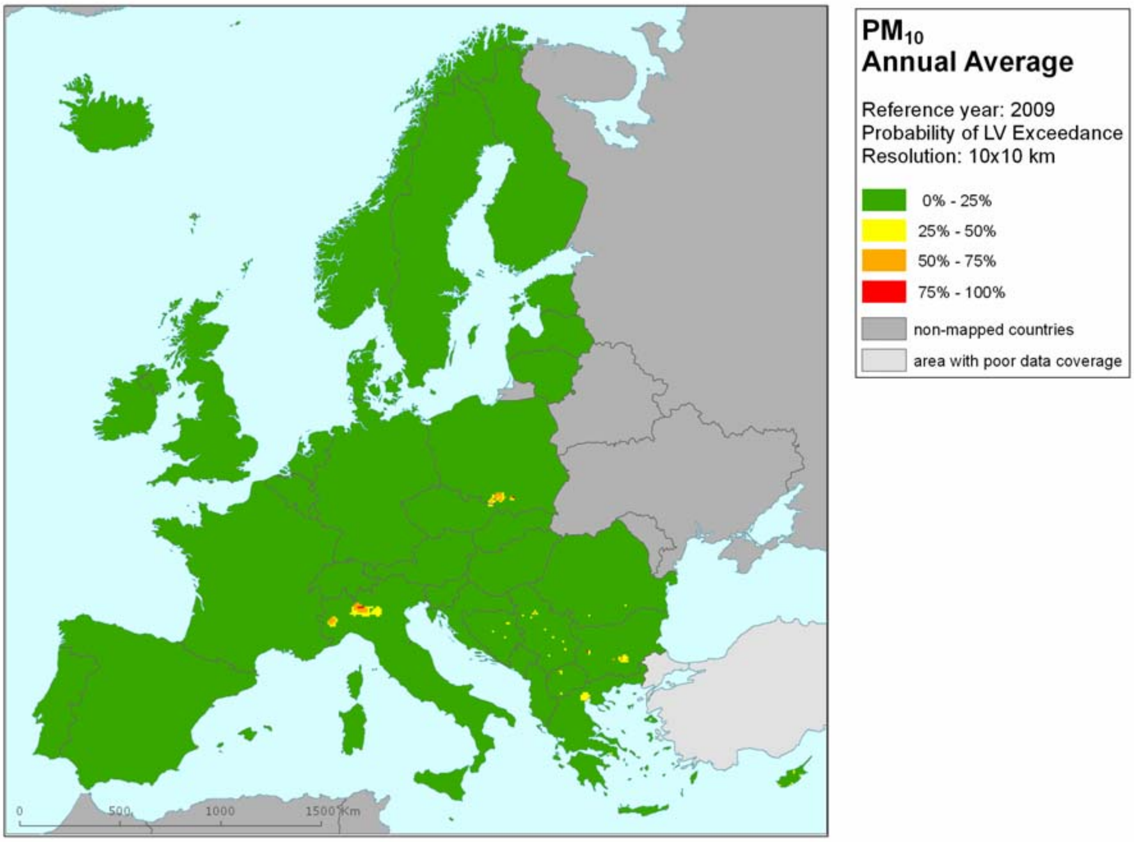

Figure 4.3 Map with the probability of the limit value exceedance for PM_{10} annual average ($\mu g.m^{-3}$) for 2009 on European scale calculated on the 10 x 10 km grid resolution. Interpolation uncertainty is considered only, no other sources of uncertainty.

4.2 36^{th} highest daily average

4.2.1 Concentration map

Similar to the PM_{10} annual average map, the combined final map of 36^{th} highest daily values has been derived from the separate rural, urban and joint rural/urban maps, using the same set of supplementary data parameters (Section 4.1.1) in the regression and its residual interpolation. Table 4.5 presents the estimated parameters of the linear regression models and of the residual kriging, including its statistical indicators.

Table 4.5 Parameters of the linear regression models (Eq.2.1) and of the ordinary kriging variograms (nugget, sill, range) - and their statistics - of PM_{10} indicator 36^{th} maximum daily mean for 2009 in the rural (left) and urban (right) areas as used for final mapping, i.e. rural linear regression model P.Eawr (left), resp. urban UP.E (right), followed by the interpolation on its regression residuals using ordinary kriging (OK, coded with 'a').

linear regr. model + OK on its residuals	rural areas (lnP.Eawr-a)	urban areas (lnUP.E-a)
	coeff.	coeff.
c (constant)	2.22	3.02
a1 (lnEMEP model 2008)	0.571	0.29
a2 (altitude GTOPO)	-0.00027	
a3 (wind speed 2006)	-0.145	
a4 (s. solar radiation 2008)	0.027	
adjusted R^2	**0.40**	**0.06**
standard error [μg.m^{-3}]	**0.28**	**0.38**
nugget	0.034	0.023
sill	0.073	0.069
range [km]	260	330
RMSE [μg.m^{-3}]	**7.96**	**13.24**
MPE [μg.m^{-3}]	**0.51**	**-0.08**

The regressions on the 2009 data have an adjusted R^2 of 0.40 for the rural areas and 0.06 for the urban areas. This fit is better than in 2008 (0.26, resp. 0.00), 2006 (0.27, resp. 0.02), 2005 (0.29, resp. 0.06), and slightly worse than the levels of the year 2007 (0.41, resp. 0.09) (De Smet et al. 2011, 2010, 2009, and Horálek et al. 2008). RMSE and MPE are the cross-validation indicators for the quality of the resulting map. Section 4.2.3 discusses in more detail the RMSE analysis and the comparison with 2008, 2007, 2006 and 2005.

Figure 4.4 presents the combined final map, where areas and stations exceeding the limit value (LV) of 50 µg.m^{-3} on more than 35 days are coloured red and purple.

As one can observe in a few areas of the map, the high measurement values do not seem to influence the interpolation results despite their clustering. The main reason is that the map presented here is on a 10 x 10 km grid resolution. Whereas, the interpolation of the separate urban and rural map took place on a 1 x 1 km grid resolution and on basis of the 1 x 1 km population density map a 1 x 1 km combined final map has been composed, for presentational purposes a 10 x 10 km aggregation has been applied. This aggregation smoothes out the elevated values one would more likely be able to distinguish in the 1 x 1 km grid map, especially in the case of urban stations representing the urban areas. The exposure estimates of Table 4.6 are derived from the 1 x 1 km map. Another less prominent reason is the smoothing effect kriging has in general. The kriging would however in case of clustering not mask these elevations in the separate 1 x 1 km urban and rural map.

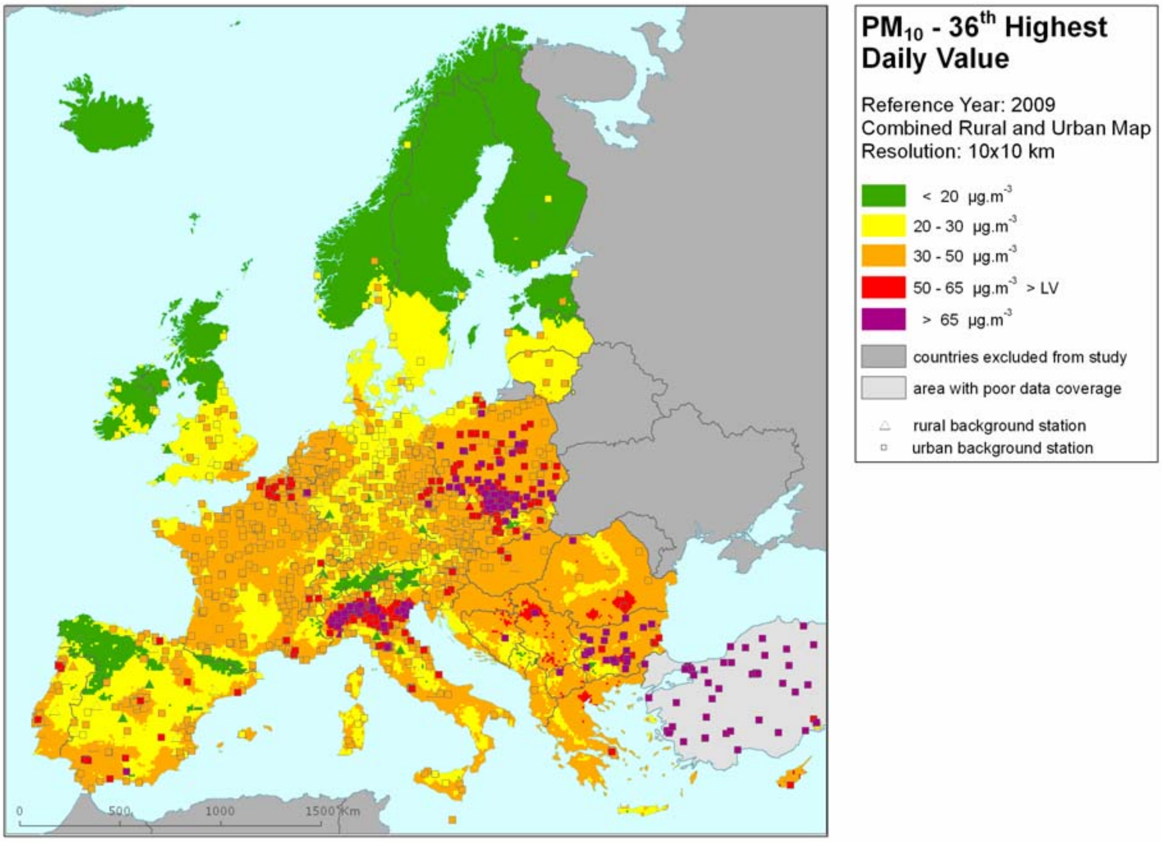

Figure 4.4 Combined rural and urban concentration map of PM_{10} – 36th maximum daily average values, year 2009. Units: µg.m^{-3}. Resolution: 10x10 km.

4.2.2 Population exposure

Table 4.6 gives the population frequency distribution for a limited number of exposure classes calculated on a 1x1 km grid resolution, as well as the population-weighted concentration for individual countries and for Europe as a whole.

Table 4.6 Population exposure and population weighted concentration – PM_{10}, 36^{th} maximum daily average value, year 2009. Resolution: 1x1 km.

Country		Population	2009 Percent [%]					Population-weighted
			< LV			> LV		
		x 1000	< 20 µg.m^{-3}	20 - 30 µg.m^{-3}	30 - 50 µg.m^{-3}	50 - 65 µg.m^{-3}	> 65 µg.m^{-3}	conc. µg.m^{-3}
Albania	AL	3 204	0	3.3	34.3	58	4	51.3
Andorra	AD	85	11.2	9.8	79.0	0	0	29.4
Austria	AT	8 355	0.9	9.2	89.9	0.0	0.0	36.7
Belgium	BE	10 753	0	1	96.0	3.3	0.0	45.8
Bosnia & Herzegovina	BA	3 760	0	5.2	29.1	21.4	44.3	57.8
Bulgaria	BG	7 607	0.0	1.6	25.0	13.7	59.7	70.3
Croatia	HR	4 435	0.000	2.4	70.0	26	2	46.9
Cyprus	CY	797	0.0	0.0	19.4	7	74	68.6
Czech Republic	CZ	10 468	0.0	3.6	81.7	9	5	43.6
Denmark	DK	5 511	0.3	95.7	4.0	0	0	26.0
Estonia	EE	1 340	30	59.7	10.5	0.0	0.0	22.4
Finland	FI	5 326	50.4	49.6	0.0	0	0	19.4
France	FR	64 369	0.1	4.3	92.6	3.0	0.0	39.2
Germany	DE	82 002	0.0	14.8	85.1	0.0	0	34.4
Greece	GR	11 260	0.0	2.4	59.3	16	22	54.7
Hungary	HU	10 031	0	0.0	75.6	24	0	46.4
Iceland	IS	319	94	6	0.0	0	0	15.8
Ireland	IE	4 450	28	72.1	0.1	0	0	21.7
Italy	IT	60 045	0	4	63.8	15	17	48.6
Latvia	LV	2 261	3.5	27.5	69.0	0.0	0.0	33.4
Liechtenstein	LI	36	0	19.4	80.3	0	0	31.5
Lithuania	LT	3 350	0.0	40.4	59.6	0.0	0.0	32.7
Luxembourg	LU	494	0.0	13.7	86.3	0	0	34.3
Macedonia, FYROM of	MK	2 049	0.0	3.0	16.7	10.2	70	75.6
Malta	MT	414	0.0	0.0	100.0	0.0	0.0	38.7
Monaco	MC	35	0	0	100.0	0.0	0	41.5
Montenegro	ME	630	1.0	19.2	14.1	52.4	13.2	51.8
Netherlands	NL	16 486	0.0	0.0	100.0	0	0	39.0
Norway	NO	4 799	28.1	46.8	25.1	0.0	0.0	24.0
Poland	PL	38 136	0.0	1.7	37.8	40	21	55.4
Portugal	PT	10 627	0.5	13.5	86.1	0	0	38.5
Romania	RO	21 499	0	1.7	58.5	33.8	6.0	49.0
San Marino	SM	32	0.0	0.0	100.0	0.0	0.0	40.6
Serbia (incl. Kosovo)	RS	9 856	0.0	1.7	20.5	16	62	67.6
Slovakia	SK	5 412	0.3	4.1	62.2	29	5	46.2
Slovenia	SI	2 032	0	0.8	99.2	0.0	0.0	41.9
Spain	ES	45 828	3	10.1	85.6	1.0	0	38.0
Sweden	SE	9 256	14.3	85.6	0.2	0.0	0.0	23.3
Switzerland	CH	7 702	0.8	7.0	91.4	1	0	37.1
United Kingdom	UK	61 595	2.7	35.9	61.4	0.0	0	30.1
Total		**536 647**	**2.0**	**13.7**	**67.8**	**9.3**	**7.2**	**41.2**
			83.5			**16.5**		

Note: Turkey is not included in the calculation due to lacking population density data.

It has been estimated that in 2009 almost 17 % of the European population lived in areas where the 36^{th} maximum daily mean of PM_{10} exceeded the limit value of 50 $\mu g.m^{-3}$. This is slightly less than in 2008 (19.4 %). However, in Albania, Bosnia-Herzegovina, Bulgaria, Cyprus, FYR of Macedonia, Montenegro, Poland, and Serbia both the population weighted indicator concentration and the median were above the LV, implicating that in these countries the average concentration per inhabitant exceeded the LV and more than half of its population was exposed to concentrations exceeding the LV. Greece has a population weighted concentration above the LV, but its median dropped well below the LV to 38 % of the population. The other countries with LV exceedances show levels that are in general reduced compared to those of 2008.

The percentage of the total European population living in areas above the LV is 16.5 % in 2009, which is 2.9 % smaller than in 2008 (19.4 %). It is well below the levels of earlier years: 2007 (22.0 %), 2006 (28.5%) and 2005 (28.1 %).

Such reduction is less obvious at the overall European population-weighted concentration of the 36^{th} maximum daily mean, which is estimated for the year 2009 at 41.2 $\mu g.m^{-3}$, being 0.1$\mu g.m^{-3}$ below that of 2008. That is about 2.5 $\mu g.m^{-3}$ lower than in 2005 (Horálek et al. 2008), about 4 $\mu g.m^{-3}$ lower than in 2006 (De Smet et al. 2009) and just 1 $\mu g.m^{-3}$ lower than in 2007 (De Smet et al. 2010).

Comparing again the observed PM_{10} exceedances in 2009 for the indicator annual average (section 4.1.2) with 36th maximum daily average, like in 2008, one can conclude that the daily limit value is the more stringent of the two.

4.2.3 Uncertainties

Uncertainty estimated by cross-validation

Cross-validation analysis determines the uncertainty. Table 4.5 shows for the combined map of PM_{10} indicator 36^{th} highest daily mean in 2009 an absolute mean uncertainty, expressed as the RMSE, of 8.0 $\mu g.m^{-3}$ for rural areas and 13.2 $\mu g.m^{-3}$ for urban areas. For previous years, the values were 8.8 and 12.7 $\mu g.m^{-3}$ (2008), 8.0 and 9.1 $\mu g.m^{-3}$ (2007), 13.3 and 9.9 $\mu g.m^{-3}$ (2006) and 9.8 and 11.7 $\mu g.m^{-3}$ (2005). It indicates that both rural and urban maps may differ from year to year somewhat in their levels of uncertainty, and that 2007 shows for both the lowest absolute uncertainty values. The relative mean uncertainty (absolute RMSE relative to the mean indicator value) of the 2009 map of PM_{10} indicator 36^{th} highest daily mean is 24.1 % for rural areas and 26.7 % for urban areas. The previous years had: 28.2 and 24.4 % (2008), 23.5 and 19.6 % (2007), 26.3 and 21.4 % (2006) and 26.6 and 23.5 % (2005). In urban areas the higher uncertainty for 2009 (and 2008), compared to their previous years is caused specifically by Turkish urban background stations reported and used in the calculations for 2008 for the first time. (An interpolation result for Turkey is not presented in the map due to lacking population density data). Table 6.4 summarises both the absolute and relative uncertainties over these past five years.

Figure 4.5 shows the cross-validation scatter plots for both rural and urban areas. The R^2 indicates that for rural areas about 56 % and for urban areas about 72 % of the variability is attributable to the interpolation. Corresponding values with those of the 2008 map (52 and 79 %), the 2007 map (60 and 65 %), the 2006 map (56 and 65 %) and the 2005 map (55 and 75 %) show that the fit is of rather average level for 2009 both types of area.

The scatter plots indicate that in areas with high concentrations the interpolation methods tend to underestimate the levels. For example, in urban areas (Figure 4.5, right panel) an observed value of 120 $\mu g.m^{-3}$ would be estimated in the interpolation as about 100 $\mu g.m^{-3}$, i.e. about 17 % too low. For rural areas, it is slightly worse.

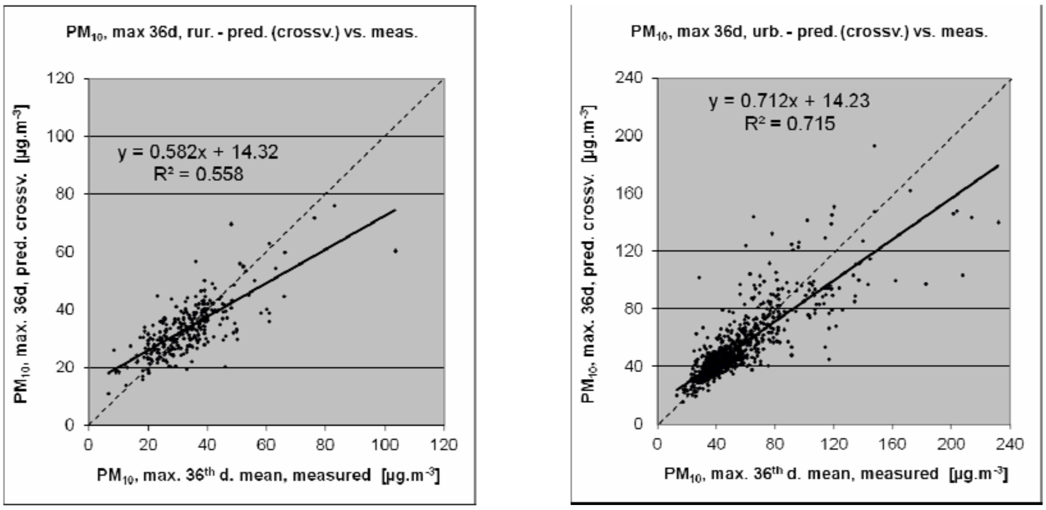

Figure 4.5 Correlation between cross-validation predicted values (y-axis) and measurements (x-axis) for the PM_{10} indicator 36^{th} maximum daily mean for 2009 for rural (left) and urban (right) areas. R^2 and the slope a (from the linear regression equation $y = a \cdot x + c$) should be as close 1 as possible, the intercept c should be as close 0 as possible.

Comparison of point measurement values with the predicted grid value

Additional to the point observation – point prediction cross-validation, a simple comparison was made between the point observation values and interpolation predicted grid values. The results of the cross-validation compared to the gridded validation are summarised in Table 4.7. The uncertainty at measurement locations is caused partly by the smoothing effect of the interpolation and partly by the spatial averaging of the values in the 10x10 km grid cells. The level of smoothing, which leads to underestimation in areas with high values, is at station locations smaller than that of the case of no measurement in such areas. For example, in urban areas the predicted interpolation gridded value will be about 88 µg.m^{-3} at the corresponding station point with the measurement value of 100 µg.m^{-3}, i.e. an underestimation of about 12 %.

Table 4.7 Linear regression equation and coefficient of determination R^2 from the scatter plots of (i) the predicted point values based on cross-validation and (ii) the aggregation into 10x10 km grid cells versus the measured point values for PM_{10} indicator 36^{th} maximum daily mean for rural and urban areas in 2009.

	rural areas		urban areas	
	equation	R^2	equation	R^2
i) cross-validation prediction (Fig 4.5)	y = 0.582x + 14.32	0.558	y = 0.712x + 14.23	0.715
ii) 10x10 km grid prediction	y = 0.704x + 9.37	0.806	y = 0.781x + 10.08	0.868

Probability of Limit Value exceedance map

Again, we constructed the map with the probability of the limit value exceedance (PoE), using an aggregated 10x10 km gridded concentration map (based on the 1x1 km combined final map of Figure 4.4), the 10x10 km gridded uncertainty map and the limit value (LV, 50 µg.m^{-3}). Figure 4.6 presents the probability of exceedance 10x10 km gridded map classifying the areas with probability of limit value exceedance below 25 % (little PoE) in green, between 25-50 % (modest PoE) in yellow, between 50-75 % (moderate PoE) in orange and above 75 % in red (large PoE). Section 4.1.3 explains in more detail the significance of the colour classes in the map.

Comparing the probability of exceedance (PoE) of 2005, 2006 and 2007, 2008 with those of 2009, one can conclude that a reduction of both the extent of areas and the elevation of its levels of likelihood of exceedances throughout Europe slows down after 2008, and slightly increased in 2009. Especially the Iberian and Italian Peninsula, Cyprus, Crete and the Balkan region do show further reduced PoE, going mostly from orange and yellow areas in 2008 to green areas in 2009. Contrary to this, for 2009 the Po valley, the southern Poland – northern Czech Republic region, some of the largest agglomerations in Greece, Bulgaria and Romania show an increased extent of area with the highest PoE (in red). Also the western Belgium and north-western France region shows increased levels of PoE, going from green in 2008 to yellow and some orange in 2009. One observes a considerably reduced likelihood of exceedances throughout Europe, except for kernels of agglomerations and regions with extended industrial activities where elevated PoE continue to exist.

Keeping in mind that the interpolated maps refer to the rural or (sub)urban background situations only, it cannot be excluded that exceedances of the limit values may occur at many *hotspot* or traffic situations throughout Europe. The increases observed in 2006 in Hungary, Romania, Bulgaria, Balkan areas, east-coast of Italy, and some coastal zones of Greece, where the PoE had gone up from yellow to orange, has been decreasing until 2009. The PoE in the urbanised regions of Rome and Naples that diminished also considerably in 2008 reduced further in 2009 to small yellow spots. The strong reduction of the PoE from 2008 to 2009 in Cyprus and to a less extent in Crete are mainly determined by just one or very few stations that showed a strong shift to measurements below the limit value.

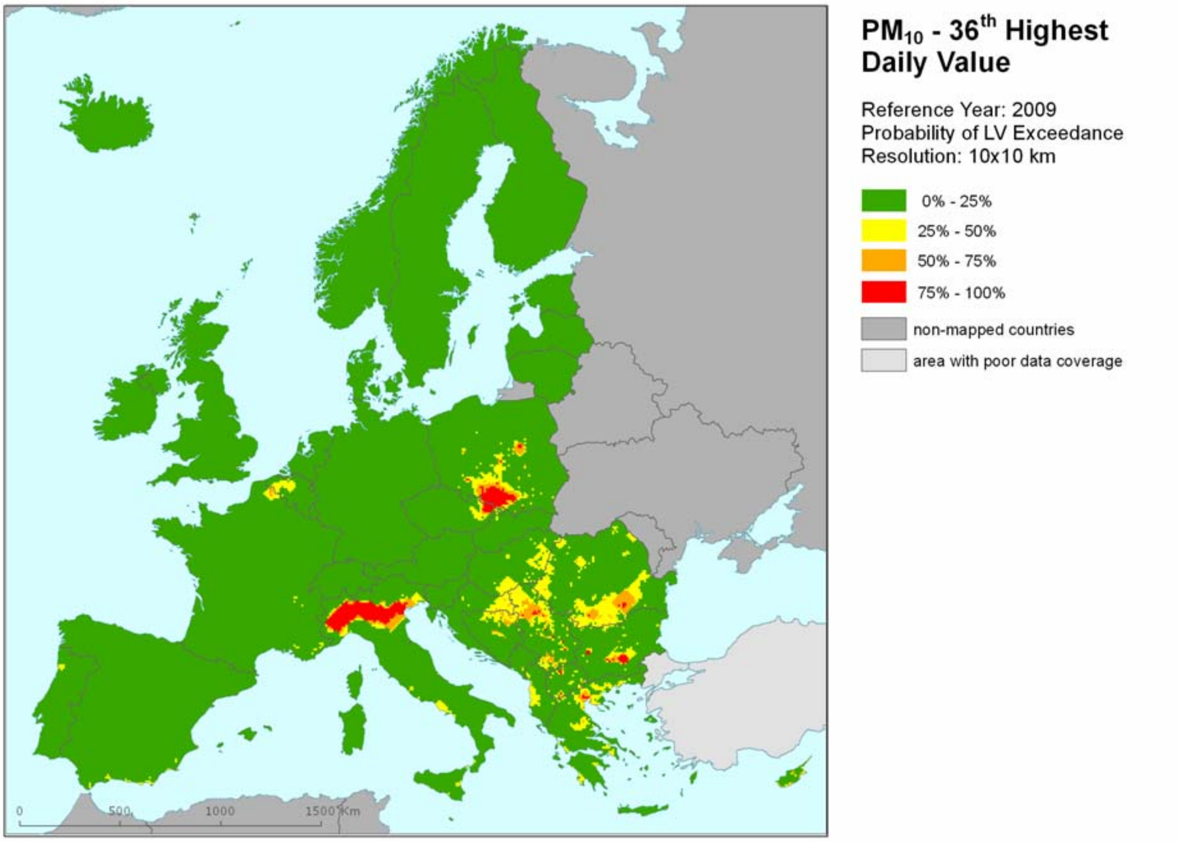

Figure 4.6 Map with the probability of the limit value exceedance for PM_{10} indicators 36^{th} maximum daily mean ($\mu g.m^{-3}$) for 2009 on the European scale calculated on the 10 x 10 km grid resolution. Interpolation uncertainty is considered only, no other sources of uncertainty.

5 Ozone maps

For ozone, the two health-related indicators 26th highest daily maximum 8-hour running mean and SOMO35, and two vegetation-related indicators AOT40 for crops and the AOT40 for forests are considered. The separate urban and rural health-related indicator fields we calculate on a 10 x10 km grid resolution. The final health-related indicator maps were created by combining rural and urban areas on basis of a 1x1 km gridded population density map, as described in Chapter 2. We present the maps on a 10x10 km grid resolution. The vegetation-related indicator maps are calculated and presented for rural areas only (assuming urban areas do not cover vegetation) and on a 2x2 km grid resolution, covering the same mapping domain as at the human health indicators. This resolution serves the needs of the EEA Core Set Indicator 005 on ecosystem exposure to ozone. As projection, we apply the standard EEA ETRS89-LAEA5210.

5.1 26th highest daily maximum 8-hour average

5.1.1 Concentration map

Figure 5.1 presents the combined final map for 26th highest daily maximum 8-hour average as result of combining the separate rural and urban interpolated map following the procedures as described in more detail in De Smet et al. (2011) and Horálek et al. (2007). Both separate maps were created by combining the measured ozone concentrations with supplementary data in a linear regression model, followed by the interpolation of its residuals by ordinary kriging. The supplementary data used in the regression model for rural areas are EMEP model output, altitude and surface solar radiation for rural areas, and EMEP model output, wind speed and surface solar radiation for urban areas, respectively. (The relevant linear regression submodels have been identified earlier as O.Ear and UO.Ewr respectively).

Table 5.1 presents the estimated parameters of the linear regression models and of the residual kriging, including the statistical indicators of both the regression and the kriging. The fit of the regression relation expressed as the adjusted R^2 is in 2009, with values of 0.59 for rural areas and 0.54 for urban areas, better than at all previous years: 2008 (0.41 and 0.43), 2007 (0.51 and 0.48), 2006 (0.40 and 0.43) and 2005 (0.45 and 0.51), (De Smet et al. 2011, 2010 and 2009, and Horálek et al. 2008). The numbers show that over the years the fit of the regressions are reasonably of the same order of magnitude at both the rural and the urban areas. RMSE and MPE are the cross-validation indicators, showing the quality of the resulting map. Section 5.1.3 discusses in more detail the RMSE analysis and comparison with results of 2009 – 2005.

Table 5.1 Parameters of the linear regression models (Eq. 2.1) and of the ordinary kriging variograms (nugget, sill, range) - and their statistics - of ozone indicator 26th highest daily maximum 8-hour mean for 2009 in the rural (left) and urban (right) areas as used the for combined final map, i.e. linear regression model O.Ear (left), resp. UO.Ewr (right) followed by interpolation of its residuals using ordinary kriging (OK, coded 'a').

linear regr. model + OK on its residuals	**rural areas (O.Ear-a)**	**urban areas (UO.Ewr-a)**
	coeff.	**coeff.**
c (constant)	12.0	43.1
a1 (EMEP model 2008)	0.82	0.61
a2 (altitude GTOPO)	0.0068	
a3 (wind speed 2008)		-3.80
a4 (s. solar radiation 2008)	0.47	0.80
adjusted R^2	**0.59**	**0.54**
standard error [µg.m^{-3}]	**9.45**	**10.52**
nugget	45	45
sill	85	76
range [km]	300	60
RMSE [µg.m^{-3}]	**8.21**	**9.32**
MPE [µg.m^{-3}]	**-0.08**	**0.09**

In the combined final map of Figure 5.1 the red and purple areas and stations do exceed the target value (TV) of 120 µg.m^{-3} (to be met by 2010). Note that in Directive 20008/50/EC the target value is defined as 120 µg/m3 not to be exceeded on more than 25 days per calendar year *averaged over three years*.

As one can observe in a few areas of the map, the high measurement values do not seem to influence the interpolation results despite their clustering. The main reason is that the map presented here is on a 10 x 10 km grid resolution. Whereas, the interpolation of the separate urban and rural map took place on a 1 x 1 km grid resolution and on basis of the 1 x 1 km population density map a 1 x 1 km combined final map has been composed, for presentational purposes a 10 x 10 km aggregation has been applied. This aggregation smoothes out the elevated values one would more likely be able to distinguish in the 1 x 1 km grid map, especially in the case of urban stations representing the urban areas. The exposure estimates of Table 5.2 are derived from the 1 x 1 km map. Another less prominent reason is the smoothing effect kriging has in general. The kriging would however in case of clustering not mask these elevations in the separate 1 x 1 km urban and rural map.

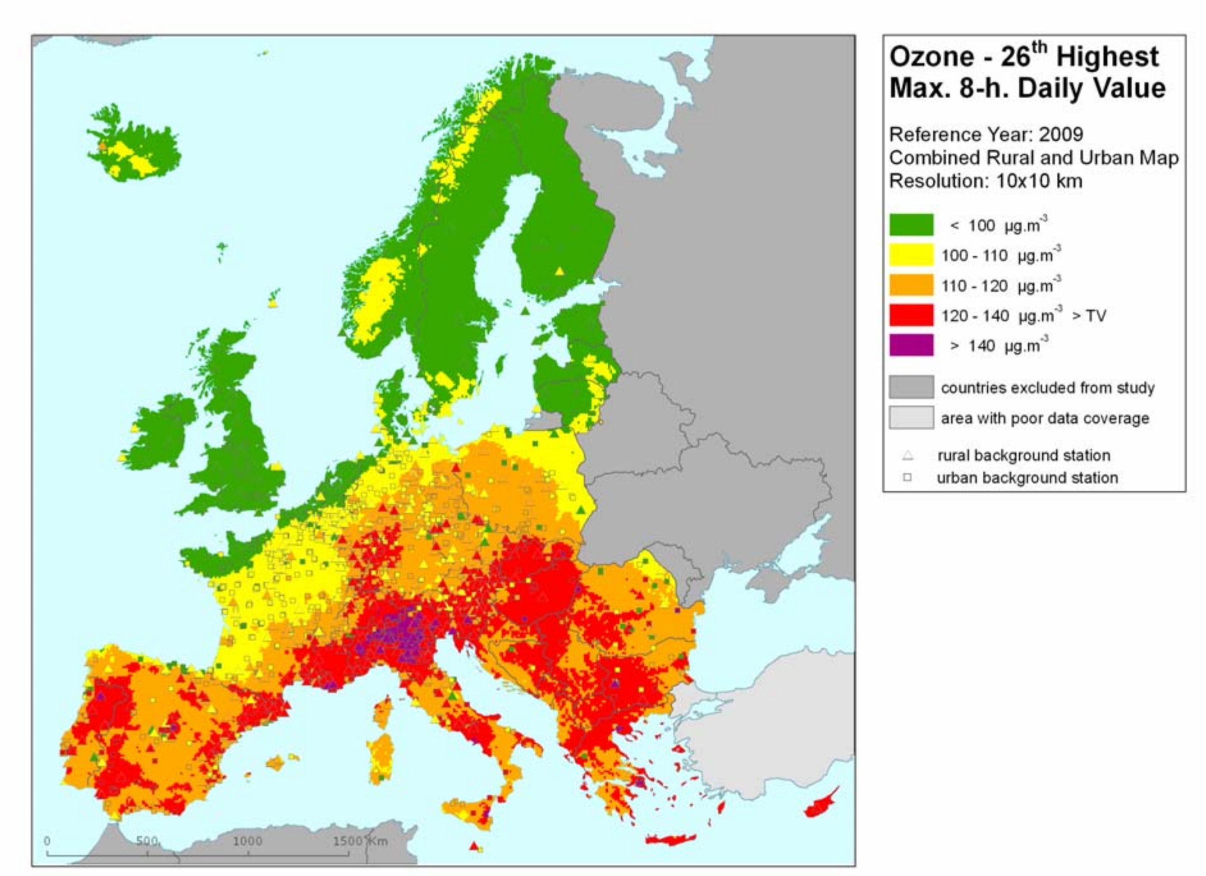

Figure 5.1 Combined rural and urban concentration map of ozone health indicators 26th highest daily maximum 8-hour value in µg.m^{-3} for the year 2009. Its target value is 120 µg.m^{-3}. Resolution: 10x10 km.

5.1.2 Population exposure

Table 5.2 gives for 26th highest daily maximum 8-hour mean the population frequency distribution for a limited number of exposure classes, as well as the population-weighted concentration for individual countries and for Europe as a whole.

Table 5.2 Population exposure and population weighted concentration – ozone, 26th highest daily maximum 8-hour mean for the year 2009.

Country		Population x 1000	2008 Percent [%] < TV < 100 µg.m-3	100 - 110 µg.m-3	110 - 120 µg.m-3	> TV 120 - 140 µg.m-3	> 140 µg.m-3	Population-weighted conc. µg.m-3
Albania	AL	3 204	0	9.8	77.0	13.2	0	114.7
Andorra	AD	85	0	0	86.5	13.5	0	115.6
Austria	AT	8 355	0	4.8	80.7	14.5	0.0	116.4
Belgium	BE	10 753	29.8	69.6	0.6	0	0	101.5
Bosnia & Herzegovina	BA	3 760	8.2	18.3	47.8	25.7	0	114.5
Bulgaria	BG	7 607	0.3	55.5	27.8	16.3	0	112.0
Croatia	HR	4 435	0	12.8	68.0	19.2	0	115.6
Cyprus	CY	797	0	0	49.1	50.9	0	120.8
Czech Republic	CZ	10 468	0	22.8	70.7	6.6	0	113.5
Denmark	DK	5 511	92.9	7.0	0.0	0	0	95.5
Estonia	EE	1 340	99.9	0.1	0	0	0	90.8
Finland	FI	5 326	100.0	0.0	0	0	0	90.6
France	FR	64 369	17.0	50.6	22.8	9.6	0	107.3
Germany	DE	82 002	3.2	62.7	32.2	2.0	0	108.8
Greece	GR	11 260	0.8	5.5	34.2	59.2	0.2	122.8
Hungary	HU	10 031	0	0	14.4	85.6	0	124.2
Iceland	IS	319	99.9	0.1	0	0	0	81.4
Ireland	IE	4 450	100	0	0	0	0	84.9
Italy	IT	60 045	0.3	8.8	33.6	38.6	18.7	125.8
Latvia	LV	2 261	94.8	5.2	0	0	0	91.9
Liechtenstein	LI	36	0	0	82.2	17.8	0	118.9
Lithuania	LT	3 350	91.2	8.8	0	0	0	95.8
Luxembourg	LU	494	0	76.7	23.3	0	0	108.6
Macedonia, FYROM of	MK	2 049	0	57.9	25.5	16.6	0	111.3
Malta	MT	414	0	93.1	6.9	0	0	107.7
Monaco	MC	35	0	0	0	100	0	127.2
Montenegro	ME	630	0	62.3	23.2	14.5	0	111.7
Netherlands	NL	16 486	85.3	14.7	0	0	0	94.7
Norway	NO	4 799	98.0	2.0	0.0	0	0	94.0
Poland	PL	38 136	11.7	47.5	40.4	0.4	0	107.8
Portugal	PT	10 627	6.2	33.1	42.2	18.5	0	112.4
Romania	RO	21 499	13.9	42.2	35.9	8.0	0	108.8
San Marino	SM	32	0	0	86.2	13.8	0	118.1
Serbia (incl. Kosovo)	RS	9 856	0	29.4	32.4	38.2	0	115.8
Slovakia	SK	5 412	0	0	11.7	88.3	0	122.7
Slovenia	SI	2 032	0	0	61.8	38.2	0	119.7
Spain	ES	45 828	9.0	19.3	53.6	18.1	0	113.1
Sweden	SE	9 256	96.6	3.4	0	0	0	94.2
Switzerland	CH	7 702	0	4.5	80.0	13.3	2.2	117.3
United Kingdom	UK	61 595	99.8	0.1	0.1	0	0	86.8
Total		**536647**	**26.1**	**29.1**	**28.9**	**13.9**	**2.1**	**108.1**
			84.0			**16.0**		

Note: Turkey is not included in the calculation due to lacking population density data.

It has been estimated that in 2009 some 16 % of the European population lived in areas where the ozone concentration exceeded the target value (TV of 120 µg.m^{-3}) of the 26th highest daily maximum 8-hour mean. This is a minor increase compared to 2008 (15 %). Similar to 2008 there are no exceedances in 2009 in the countries of the Benelux and Scandinavia, the UK, Ireland and Iceland. Countries with a similar number of inhabitants in 2008 and 2009 submitted to exposures exceeding the target value are Czech Republic (7 %), Spain (17 %) and the small states with none or few measurement stations Andorra (14 %), San Marino (14 %), and Monaco (100 %). The population weighted concentration of Monaco is in 2009 above the target value.

Increases in countries are observed for 2009 compared to 2008 and can be categorized into three cases.

- Countries with population exposures above the TV in 2008 that show an increase in 2009, but still do not concern more than 1/5th of the national population: countries of the Alpine region, Romania, Bulgaria and most Balkan countries, with the exception of Slovenia and Serbia (with both 38 % of their population exposure in excess in 2009).
- Remarkably steep increases in the percentage of national population exposed, going from below the median in 2008 to above the median in 2009, do occur in Cyprus (from <1 % in 2008 to 51 % in 2009), Hungary (from 29 to 86 %) and Slovakia (from 24 to 88 %). Hungary and Slovakia did show in 2009 population weighted concentrations above the TV.
- There is one country, Italy, where more than half of the population was exposed to levels above the TV both in 2008 (55 %) and in 2009 (56 %). Italy had in 2009 a population weighted concentration above the TV.

For the decreases in national population exposures of 2009 compared to those of 2008, one observes three cases as well.

- Despite a decrease, more than half of the population was in 2009 still exposed to levels above the TV in Greece (from 75 % in 2008 down to 60 % in 2009), with a population weighted concentration above the TV.
- Countries with more than half of their population living above the TV in 2008 exhibiting significant decreases in 2009: the Balkan countries Albania (form 78 to 13 %) and FYR of Macedonia (from 70 to 17 %). This can be under influence from the limited number of observations in these countries.
- Countries well below the median of its population exposed to TV exceedances in 2008 showing a significant decrease in 2009 to almost non-exceedance: Germany (from 11 % in 2008 to 2 % in 2009), Malta (from 2 % to no exceedance in 2009) and Poland from 2 to 0.5 %.

The average concentration per inhabitant (i.e. population weighted concentration) of Cyprus, Greece, Hungary, Italy, Monaco, and Slovakia has been estimated for 2009 to be above the target value, with about 51 % of the Cypriots, 56 % of the Italians, some 60 % of the Greek, more than 85 % of the Hungarian and Slovakian population, and all citizens of Monaco being exposed to average levels above the TV. Albania and FYR of Macedonia that had a population weighted concentration above the TV in 2008 show in 2009 values well below the TV. Greece has a lower population weighted concentration in 2009 than in 2008, but it was still above the TV. Cyprus, Hungary and Slovakia had an increase from levels below the TV in 2008 to levels above the TV in 2009. Italy and Monaco had in 2008 a population weighted concentration above the TV, which further increased in 2009. Part of the population in Greece (0.2 %) and Switzerland (2 %) and more substantially in Italy (almost 19 %) were estimated to be exposed to ozone levels of more than 140 $\mu g.m^{-3}$. As the current mapping methodology tends to underestimate high values due to interpolation smoothing, these actual numbers will most likely be higher. The Iberian Peninsula shows for 2009, compared to 2008, an increase in exposure levels over the full range of <100–140 $\mu g.m^{-3}$. Most of the other countries without population weighted exceedances showed a decrease in their population weighted concentrations in 2009 compared to 2008.

The overall European population-weighted ozone concentration in terms of the 26th highest daily maximum 8-hour mean was estimated for the year 2009 to 108 $\mu g.m^{-3}$. That is a decrease compared to previous years.

5.1.3 Uncertainties

Uncertainty estimated by cross-validation

The basic uncertainty analysis is given by cross-validation. Table 5.1 shows RMSE values of 8.2 $\mu g.m^{-3}$ for the rural areas and 9.3 $\mu g.m^{-3}$ for the urban areas of the combined final map. For previous years the values were for rural and urban areas respectively: 8.7 and 8.8 $\mu g.m^{-3}$ (2008), 8.8 and 8.9

µg.m^{-3} (2007), 11.2 and 10.2 µg.m^{-3} (2006), and 12.3 and 10.0 µg.m^{-3} (2005) (De Smet et al. 2011, 2010 and 2009, Table 5.1; Horálek et al. 2008, Tables A3.3, A3.12). It could indicate a reduction in uncertainty over time in the rural areas, which does not occur in the urban areas. The relative mean uncertainty of the 2009 ozone map is 7.2 % for rural areas and 8.4 % for urban areas. The previous years had for rural and urban areas respectively: 7.6 % and 7.9 % (2008), 7.5 % and 7.9 % (2007), 8.9% and 8.4 % (2006), 10.3 %, and 8.9 % (2005). Table 6.5 summarises both the absolute and relative uncertainties over these past five years.

Figure 5.2 shows the cross-validation scatter plots for both the rural and urban areas of the 2009 map. The R^2, an indicator for the interpolation correlation with the observations, shows that for the rural areas about 69 % and for the urban areas about 64 % of the variability is attributable to the interpolation. Corresponding values for the 2008 map (56 % and 61 %), 2007 map (71 % and 66 %), the 2006 map (49 % and 53 %) and the 2005 map (51 % and 50 %), show a fit at both the rural and urban interpolations in line with the levels of 2007 being higher than the years 2005, 2006 and 2008.

The scatter plots indicate that the higher values are underestimated and the lower values somewhat overestimated by the interpolation method; a typical smoothing effect inherent to interpolation method of the linear regression and its residuals kriging. For example, in rural areas (Figure 5.2, left panel) an observed value of 150 µg.m^{-3} is estimated in the interpolation as 137 µg.m^{-3}, which is 9 % too low.

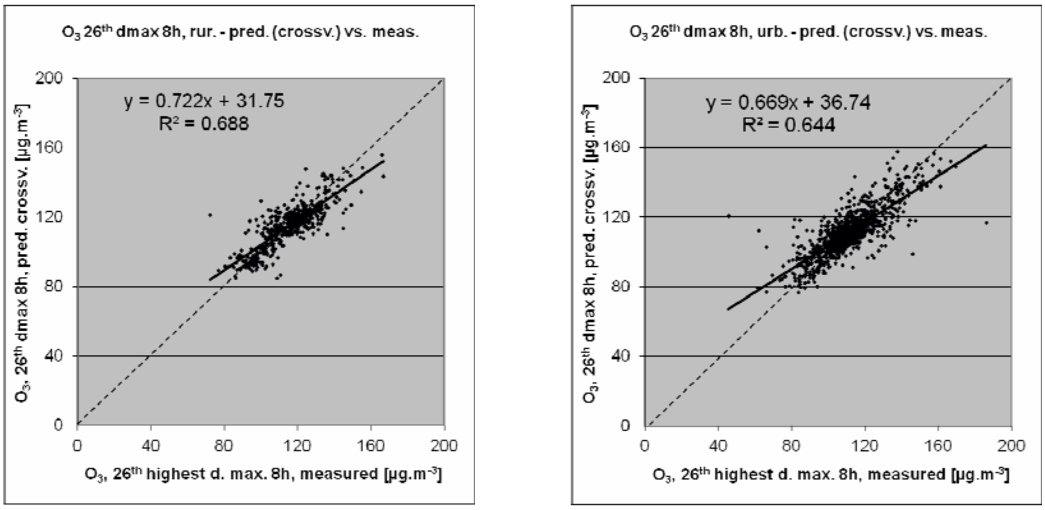

Figure 5.2 Correlation between cross-validation predicted values (y-axis) and measurements (x-axis) for the ozone indicator 26th highest daily maximum 8-hour mean for rural (left) and urban (right) areas in 2009.

Comparison of point measurement values with the predicted grid value

Additional to the point observation - point prediction cross-validation, a simple comparison was made between the point observation values and interpolated predicted grid values. The results of the cross-validation compared to the gridded validation examination are summarised in Table 5.3. The uncertainty at measurement locations is caused partly by the smoothing effect of interpolation and partly by the spatial averaging of the values in the 10x10 km grid cells. The level of smoothing effect leading to underestimation at areas with high values is here smaller in case no measurement is present in such areas. For example, in rural areas the predicted interpolation grid value will be about 140 µg.m^{-3} at the corresponding station point with the observed value of 150 µg.m^{-3}, i.e. an underestimation of about 7 %.

Table 5.3 Linear regression equation and coefficient of determination R^2 from the scatter plots of (i) the predicted point values based on cross-validation and (ii) aggregation into 10x10 km grid cells versus the measured point values for the ozone indicator 26th highest daily maximum 8-hour mean for rural and urban areas of 2009.

	rural areas		urban areas	
	equation	R^2	equation	R^2
i) cross-validation prediction (Fig 5.2)	y = 0.722x + 31.75	0.688	y = 0.669x + 36.74	0.644
ii) 10x10 km grid prediction	y = 0.794x + 23.54	0.833	y = 0.762x + 26.48	0.825

Probability of Target Value exceedance map

A 10x10 km gridded map with the probability of the target value exceedance in Figure 5.3 has been constructed on the basis of the 10x10 km gridded concentration map (Figure 5.1) as aggregation of the 1x1 km gridded map, the 10x10 km gridded uncertainty map and the target value (TV) of 120 µg.m^{-3}. Section 4.1.3 explains the significance of the colour classes in the map.

Comparing 2009 with 2008 – 2005 it becomes evident that after the year 2006 with its temporal increase in PoE to levels above 50 % and even above 75 % in large parts of specifically central Europe, a continued decrease took place in the levels of PoE in 2009 – 2007, to levels in many areas well below those of 2005. In 2009, most of the red areas (large PoE) in the southern and central regions of Europe did however not change compared to 2008. On the contrary the red areas extended somewhat. One can observe this most clearly in the wider area of and around the Po Valley and its extensions up to the Alps.

In eastern/south-eastern Europe were clear increases, going yellow to orange (moderate PoE) and from orange to red (large PoE), but less extended than in 2007. On the Iberian Peninsula enlarged areas were estimated with large PoE (red) at and around urban agglomerations. Reductions were observed in the northern part of central Europe where the yellow (modest PoE) of 2008 turned into green (little PoE) in 2009.

The meteorologically induced variations from year to year, combined with methodological uncertainties and the limited number of years considered here do not allow for conclusions on any significant tendency. For that purpose, one would need longer time series and reduced uncertainties.

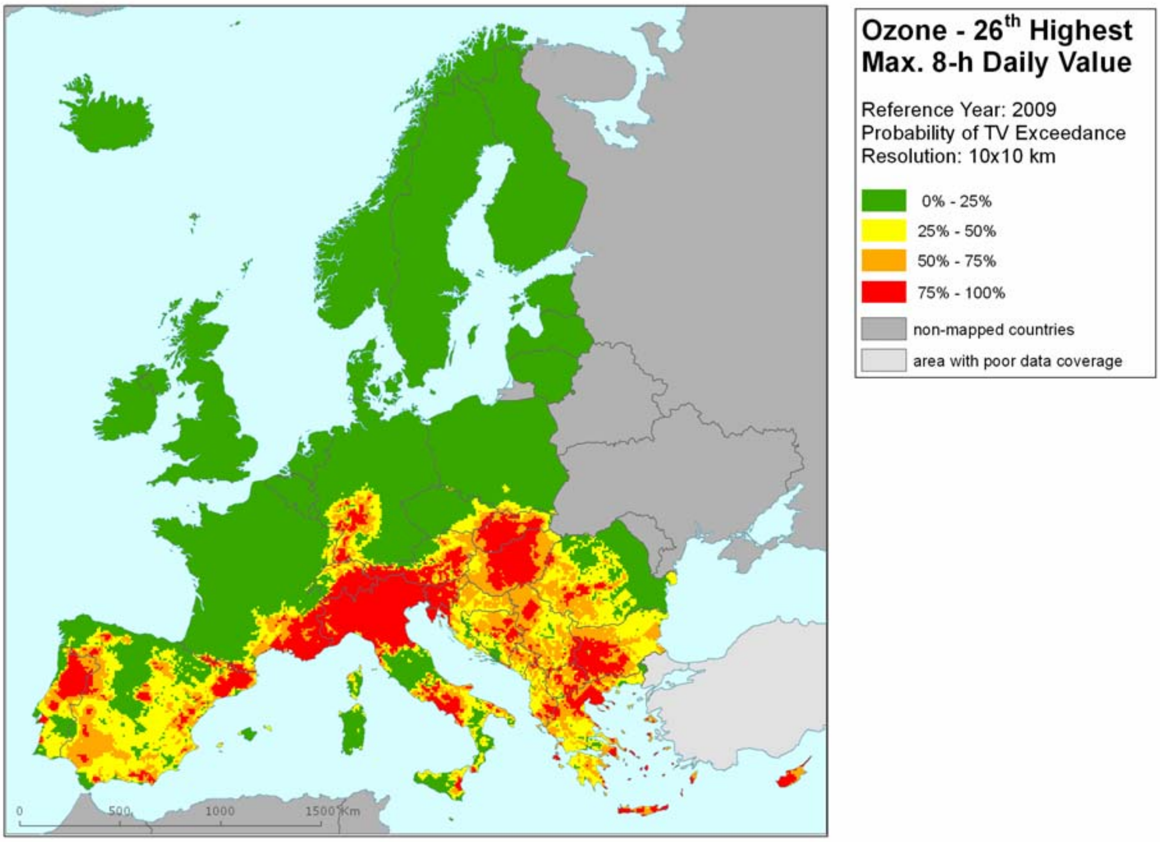

Figure 5.3 Map with the probability of the target value exceedance for ozone indicator 26th highest daily maximum 8-hour average (µg.m^{-3}) for 2009 on European scale calculated on the 10 x 10 km grid resolution. Interpolation uncertainty is considered only, no other sources of uncertainty.

5.2 SOMO35

5.2.1 Concentration map

Figure 5.4 presents the combined final map for SOMO35 as result of combining the separate rural and urban interpolated map following the procedure as described in De Smet et al. (2011) and Horálek et al. (2007).

As one can observe in a few areas of the map, the high measurement values do not seem to influence the interpolation results despite their clustering. The main reason is that the map presented here is on a 10 x 10 km grid resolution. Whereas, the interpolation of the separate urban and rural map took place on a 1 x 1 km grid resolution and on basis of the 1 x 1 km population density map a 1 x 1 km combined final map has been composed, for presentational purposes a 10 x 10 km aggregation has been applied. This aggregation smoothes out the elevated values one would more likely be able to distinguish in the 1 x 1 km grid map, especially in the case of urban stations representing the urban areas. (The exposure estimates of Table 5.5 are derived from the 1 x 1 km map). Another less prominent reason is the smoothing effect kriging has in general. The kriging would however in case of clustering not mask these elevations in the separate 1 x 1 km urban and rural map.

The supplementary data used in the regression models are the same as for 26th highest daily maximum 8-hour mean, i.e. EMEP model output, altitude and surface solar radiation for rural areas and EMEP model output, wind speed and surface solar radiation for urban areas. (The relevant linear regression submodels are identified as O.Ear, resp. UO.Ewr.)

Table 5.4 presents the estimated parameters of the linear regression models and of the residual kriging, including the statistical indicators of both the regression and the kriging. The fit of the regression is expressed by the adjusted R^2 and standard error. The adjusted R^2 is in 2009 for the rural areas 0.60 and for the urban areas 0.53. This is a somewhat better fit than in 2008 (0.49 and 0.44) and quite similar to 2007 (both 0.58) and 2005 (0.51 and 0.49), but slightly better than 2006 (0.42 and 0.38), (De Smet et al. 2011 and 2010, Table 5.4; Horálek et al. 2008, Tables A3.1 and A3.11). RMSE and MPE are the cross-validation indicators showing the quality of the resulting map. Section 5.2.3 discusses in more detail the RMSE analysis and comparison with results of 2008, 2007, 2006 and 2005.

Table 5.4 Parameters of the linear regression models (Eq. 2.1) and of the ordinary kriging variograms (nugget, sill, range) - and their statistics - of ozone indicator SOMO35 for 2009 in the rural (left) and urban (right) areas as used for final mapping, i.e. rural linear regression model O.Ear (left), resp. UO.Ewr (right) followed by the interpolation on its residuals using ordinary kriging (OK, coded with 'a').

linear regr. model + OK on its residuals	rural areas (O.Ear-a)	urban areas (UO.Ewr-a)
	coeff.	coeff.
c (constant)	-991	-602
a1 (EMEP model 2008)	0.66	0.52
a2 (altitude GTOPO)	1.16	
a3 (wind speed 2008)		-226.69
a4 (s. solar radiation 2007)	155.76	207.88
adjusted R^2	**0.60**	**0.53**
standard error [μg.m^{-3}.d]	**1701**	**1630**
nugget	2.2E+06	1.3E+06
sill	2.8E+06	1.7E+06
range [km]	290	190
RMSE [μg.m^{-3}.d]	**1635**	**1475**
MPE [μg.m^{-3}.d]	**-14**	**-1**

SOMO35 is not subject to one of the EU air quality directives and there is no limit or target values defined, which does not allow for mapping the probability of exceedances.

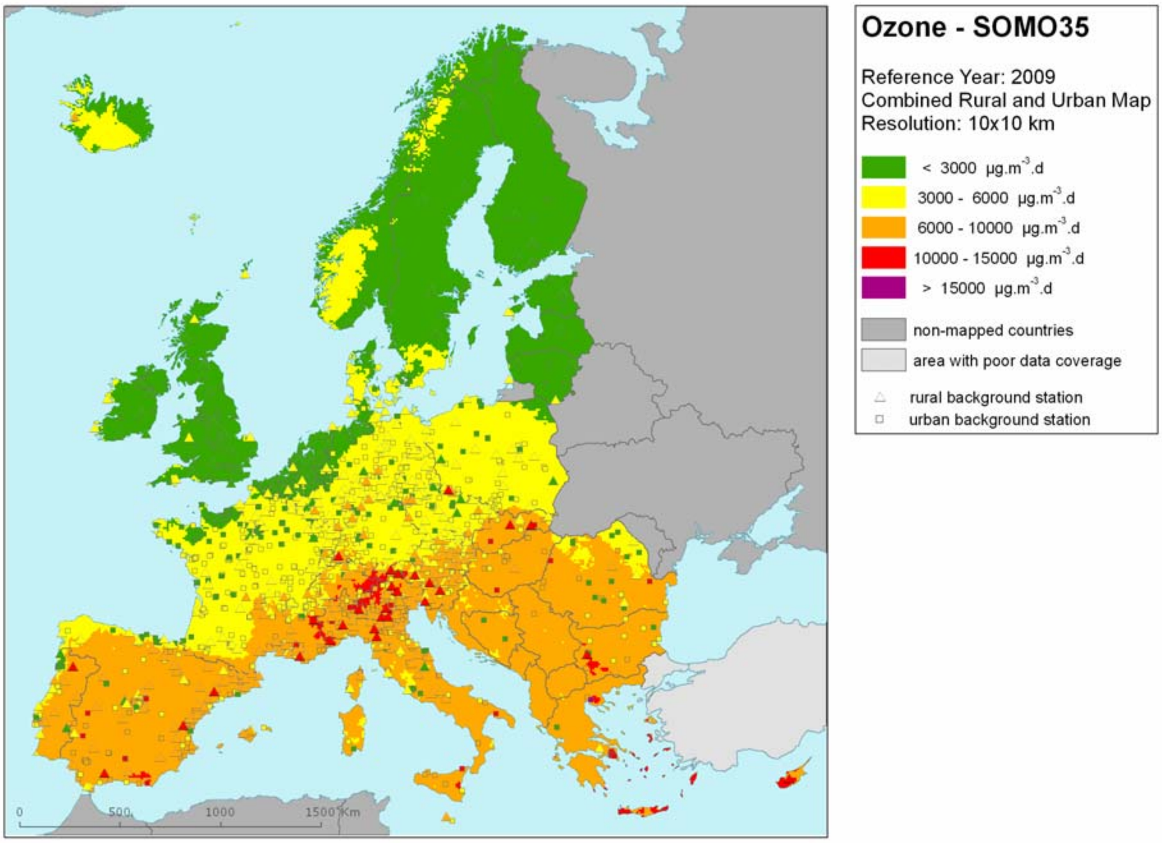

Figure 5.4 Combined rural and urban concentration map of ozone indicators SOMO35 in µg.m^{-3}.days for the year 2009. Resolution: 10x10 km.

5.2.2 Population exposure

Table 5.5 gives for SOMO35 the population frequency distribution for a limited number of exposure classes, as well as the population-weighted concentration for individual countries and for Europe as a whole.

It has been estimated that in 2009 almost 25 % of the European population lived in areas with SOMO35 values above 6000 µg.m^{-3}.d. This is an increase of 5 % compared to 2008. Many of the northern and north-western European countries had a rather similar number of people living in 2008 in areas submitted to more than 6000 µg.m^{-3}.d. Others do show increases or decreases of different extents and ranges, and rather scattered from country to country. In Greece, Albania, Cyprus, Malta, Andorra and Monaco almost all people were exposed to this level as they did in 2008. In Italy and Serbia, more than half of the population continued to be exposed to levels above 6000 µg.m^{-3} in 2009. In Spain, Slovakia and Hungary a steep increase of the number of people exposed was observed, from around a quarter to one-third in 2008 to almost two-thirds, and in Hungary 90 %.

Comparing the national frequency distribution of 2009 with that of 2008, one observes shifts in the number of inhabitants per class per country that coincide more or less with the shifts in colour classes per country in the maps of 2008 and 2009.

We observe in 2009 compared to 2008 a slight (further) European overall decrease in population exposed to ozone levels above 10 000 µg.m^{-3}.d. In 2009 limited areas of, Austria, Bulgaria, Greece, Italy, Switzerland and a more considerable part of Cyprus exhibit these elevated SOMO35 values (red grids in the map).

Table 5.5 Population exposure and population weighted concentration – ozone, SOMO35, year 2009.

Country		Population x1000	2008 Percent [%] < 3000 µg.m^{-3}.d	3000 - 6000 µg.m^{-3}.d	6000 - 10000 µg.m^{-3}.d	10000 - 15000 µg.m^{-3}.d	> 15000 µg.m^{-3}.d	Population-weighted conc. µg.m^{-3}.d
Albania	AL	3 204	0	2.4	97.6	0	0	6754
Andorra	AD	85	0	0	100	0	0	7186
Austria	AT	8 355	0	86.6	13.3	0.1	0	5050
Belgium	BE	10 753	90.8	9.2	0	0	0	2599
Bosnia & Herzegovina	BA	3 760	0	66.2	33.8	0	0	5536
Bulgaria	BG	7 607	0	67.3	32.3	0.4	0	5686
Croatia	HR	4 435	0	67.5	32.5	0	0	5491
Cyprus	CY	797	0	0	92.4	7.6	0	8788
Czech Republic	CZ	10 468	0	99.2	0.8	0	0	4487
Denmark	DK	5 511	84.0	16.0	0	0	0	2440
Estonia	EE	1 340	99.8	0.2	0	0	0	1762
Finland	FI	5 326	100.0	0.0	0	0	0	1623
France	FR	64 369	27.8	59.0	13.2	0.0	0	4025
Germany	DE	82 002	24.7	74.9	0.4	0	0	3507
Greece	GR	11 260	0	1.2	95.8	3.0	0	8330
Hungary	HU	10 031	0	10.1	89.9	0	0	6631
Iceland	IS	319	95.6	4.4	0	0	0	833
Ireland	IE	4 450	98.6	1.4	0	0	0	1487
Italy	IT	60 045	0	24.7	74.9	0.4	0	6986
Latvia	LV	2 261	100.0	0.0	0	0	0	1837
Liechtenstein	LI	36	0	87.8	12.2	0	0	5271
Lithuania	LT	3 350	99.6	0.4	0	0	0	2291
Luxembourg	LU	494	0	100	0	0	0	3500
Macedonia, FYROM of	MK	2 049	0	58.5	41.5	0.0	0	6229
Malta	MT	414	0	0	100	0	0	6634
Monaco	MC	35	0	0	100	0	0	8325
Montenegro	ME	630	0	62.9	37.1	0	0	6237
Netherlands	NL	16 486	99.7	0.3	0	0	0	1922
Norway	NO	4 799	96.2	3.8	0	0	0	2000
Poland	PL	38 136	17.6	81.9	0.5	0	0	3747
Portugal	PT	10 627	6.7	64.4	28.9	0	0	5003
Romania	RO	21 499	0.6	71.1	28.3	0	0	5044
San Marino	SM	32	0	84.7	15.3	0	0	5860
Serbia	RS	9 856	0	39.4	60.6	0	0	6118
Slovakia	SK	5 412	0	24.4	75.6	0	0	6348
Slovenia	SI	2 032	0	63.4	36.6	0	0	5775
Spain	ES	45 828	7.9	34.3	57.7	0.0	0	5983
Sweden	SE	9 256	96.0	4.0	0	0	0	2100
Switzerland	CH	7 702	0	85.7	14.0	0.3	0	5139
United Kingdom	UK	61 595	99.4	0.6	0	0	0	1433
Total		**536647**	**31.9**	**43.5**	**24.5**	**0.1**	**0.0**	**4275**
			75.4		**24.6**			

Note: Turkey is not included in the calculation due to lacking population density data.

The total European population-weighted ozone concentration in terms of SOMO35 was estimated as 4275 µg.m^{-3}.d which is the same value as in the previous year 2008 (4275 µg.m^{-3}.d).

5.2.3 Uncertainties

Uncertainty estimated by cross-validation

The basic uncertainty analysis is given by cross-validation. In Table 5.4 the absolute mean uncertainty (RMSE) in 2009 is 1635 µg.m^{-3}.d for the rural areas and 1475 µg.m^{-3}.d for the urban areas. This means that at the rural areas the improvement in uncertainty reduction compared to its previous years is confirmed, but not at the urban areas where 2009 shows its highest uncertainty level of all years. The uncertainties at rural and urban areas in previous years are: 1609 (rural areas and 1293 µg.m^{-3}.d (2008), 1801 and 1260 µg.m^{-3}.d (2007), 2077 and 1472 µg.m^{-3}.d (2006) and 2173 and 1459 µg.m^{-3}.d (2005). The relative mean uncertainty of the 2009 map of SOMO35 is 29.7 % for rural areas and 33.1 % for urban areas. The previous years had for rural and urban areas respectively: 30.7 % and 31.3 % (2008), 33.3 % and 29.5 % (2007), 31.6 % and 29.2 % (2006), and 35.5 % and 32 % (2005), meaning that the 2009 relative uncertainties are for rural at the lower end and for urban at the higher end of the range of years. Table 6.5 summarises both the absolute and relative uncertainties over these past five years.

Figure 5.5 shows the cross-validation scatter plots for interpolated values at both rural and urban areas. R^2 indicates that in 2009 for the rural areas about 63 % and for the urban areas about 62 % of the variability is attributable to the interpolation. The corresponding values for the 2008 maps (63 % and 54 %), 2007 maps (63 % and 67 %), the 2006 maps (47 % and 49 %) and 2005 maps (55 % and 58 %), illustrate a quite equal fit in 2009 at both rural and urban areas and a somewhat similar fit at rural areas for the years 2009 – 2007.

The scatter plots show again that in areas with high concentrations the interpolation methods tend to deliver underestimated predicted values, with additionally at the urban areas at the lower values some overestimation. For example, in urban areas (Figure 5.5, right panel) an observed value of 10 000 µg.m^{-3}.d is estimated in the interpolation as about 7900 µg.m^{-3}.d. That is 21 % too low, leading in general to high underestimations at high SOMO35 values. Vice versa at low values an overestimation will occur, e.g. at a measured 2000 µg.m^{-3}.d the interpolation will predict some 2900 µg.m^{-3}.d, which is about 45 % too high.

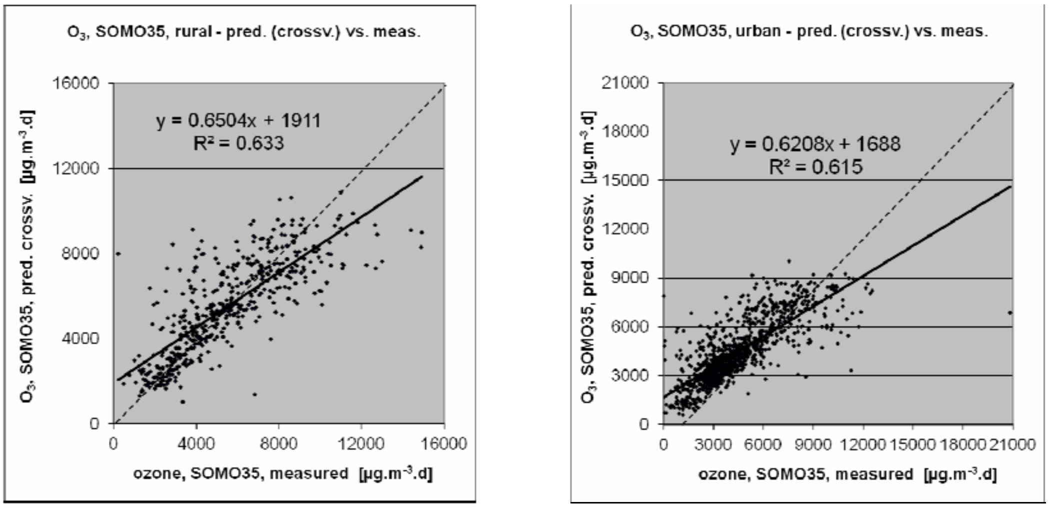

Figure 5.5 Correlation between cross-validation predicted values (y-axis) and measurements (x-axis) for the ozone indicator SOMO35 for rural (left) and urban (right) areas in 2009.

Comparison of point measurement values with the predicted grid value

Additional to the point observation - point prediction cross-validation, a simple comparison was made between the point measurements and interpolated predicted grid values averaged in a 10x10 km grid for the separate rural and urban map. This point-grid comparison indicates to what extent the predicted value of a grid cell represents the corresponding measured values at stations located in that cell. The results of the point observation - point prediction cross-validation of Figure 5.5, compared to those of the point-grid validation are summarised in Table 5.6. The table shows a better correlated relation (i.e. higher R^2, smaller intercept and slope closer to 1) between station measurements and the interpolated values of the corresponding grid cells (case ii) at both rural and urban map areas than it does at the point cross-validation predictions (case i). That is because the simple comparison between point measurements and the gridded interpolated values shows the uncertainty at the actual station locations (points) itself, while the point observation – point prediction cross-validation simulates the behaviour of the interpolation at positions without actual measurements within the area covered by measurements. The uncertainty at measurement locations is caused partly by the smoothing effect of the interpolation and partly by the spatial averaging of the values in the 10x10 km grid cells. The level of the smoothing effect leading to underestimation in areas with high values is there smaller than it is in case no measurement is performed in such areas. For example, in urban areas the predicted interpolation grid value will be about 8300 $\mu g.m^{-3}.d$ at the corresponding station point with the observed value of 10 000 $\mu g.m^{-3}.d$, i.e. an underestimation of about 17 %.

Table 5.6 Linear regression equation and coefficient of determination R^2 from the scatter plots of (i) the predicted point values based on cross-validation and (ii) aggregation into 10x10 km grid cells versus the measured point values for the ozone indicator SOMO35 for rural and urban areas of 2009.

	rural areas		urban areas	
	equation	R^2	equation	R^2
i) cross-validation prediction (Fig 5.5)	y = 0.650x + 1911	0.633	y = 0.621x + 1688	0.615
ii) 10x10 km grid prediction	y = 0.706x + 1606	0.741	y = 0.630x + 1355	0.730

No Limit Value or Target Value is set for the WHO recommended ozone health indicator SOMO35, therefore no probability of exceedance map has been prepared.

5.3 AOT40 for crops and for forests

The ecosystem based accumulative ozone indicators described in this section are specifically intended for insertion in the EEA Core Set of Indicator 005 (CSI005, http://themes.eea.europa.eu/indicators). For the estimation of the vegetation and forest land areas exposures to accumulated ozone the maps in this section are created on a 2x2 km grid, instead of the 10x10km grid resolution used to calculate the separate rural and urban maps for the human health indicators. This resolution is selected as a compromise between calculation time and accuracy in the impact analysis done for the ozone impact assessment of the CSI005, which uses results of this section. It serves as a refinement of the exposure frequency distribution outcomes of the overlay with the 100x100 m resolution CLC2000 land cover classes.

5.3.1 Concentration maps

The interpolated maps for AOT40 for crops and AOT40 for forests were created for rural areas only, combining AOT40 data derived from rural background station observations with the supplementary data sources EMEP model output, altitude and surface solar radiation. (The relevant linear regression submodel is identified as O.Ear.). Note that supplementary data sources are the same as for the human health related ozone indicators.

Table 5.7 presents the estimated parameters of the linear regression models and of the residual kriging, including their statistical indicators of the regression and kriging. The fit of the regression is expressed by adjusted R^2 and the standard error. The adjusted R^2 is in 2009 for AOT40 for crops 0.64 and for AOT40 for forests 0.61, i.e. better fit than in 2008 (0.40 and 0.49) and in 2007 (0.49 and 0.59) (De Smet et al. 2011 and 2010, Table 5.7). RMSE and MPE are the cross-validation indicators, showing the quality of the resulting map. Section 5.3.3 discusses in more detail the RMSE analysis and comparison with results of 2008, 2007, 2006 and 2005.

Table 5.7 Parameters of the linear regression models (Eq2.1) and of the ordinary kriging variograms (nugget, sill, range) - and their statistics - of ozone indicators AOT40 for crops (left) and for forests (right) for 2009 in the rural areas as used for final mapping, i.e. rural linear regression model O.Ear followed by the interpolation on its residuals using ordinary kriging (OK, coded with 'a').

linear regr. model + OK on its residuals	**AOT40 for crops (O.Ear-a)**	**AOT40 for forests (O.Ear-a)**
	coeff.	**coeff.**
c (constant)	-7868	-12201
a1 (EMEP model 2008)	0.78	0.58
a2 (altitude GTOPO)	1.86	6.76
a3 (s. solar radiation 2008)	872.5	1651.6
adjusted R^2	**0.64**	**0.61**
standard error [µg.m^{-3}]	**5556**	**10221**
nugget	1.2E+07	3.6E+07
sill	3.4E+07	7.2E+07
range [km]	470	470
RMSE [µg.m^{-3}]	**5138**	**9304**
MPE [µg.m^{-3}]	**-67**	**-137**

Figure 5.6 presents the final map of AOT40 for crops. The areas and stations in the map that exceed the target value (TV) of 18 mg.m^{-3}.h are marked in red and purple. It concerns a map for rural areas, just based on rural background station observations, representing an indicator for vegetation exposure to ozone while assuming there is no relevant vegetation in the urban areas.

The same holds for the final rural map of AOT40 for forests as presented in Figure 5.7. However, for AOT40 for forests there is no TV defined.

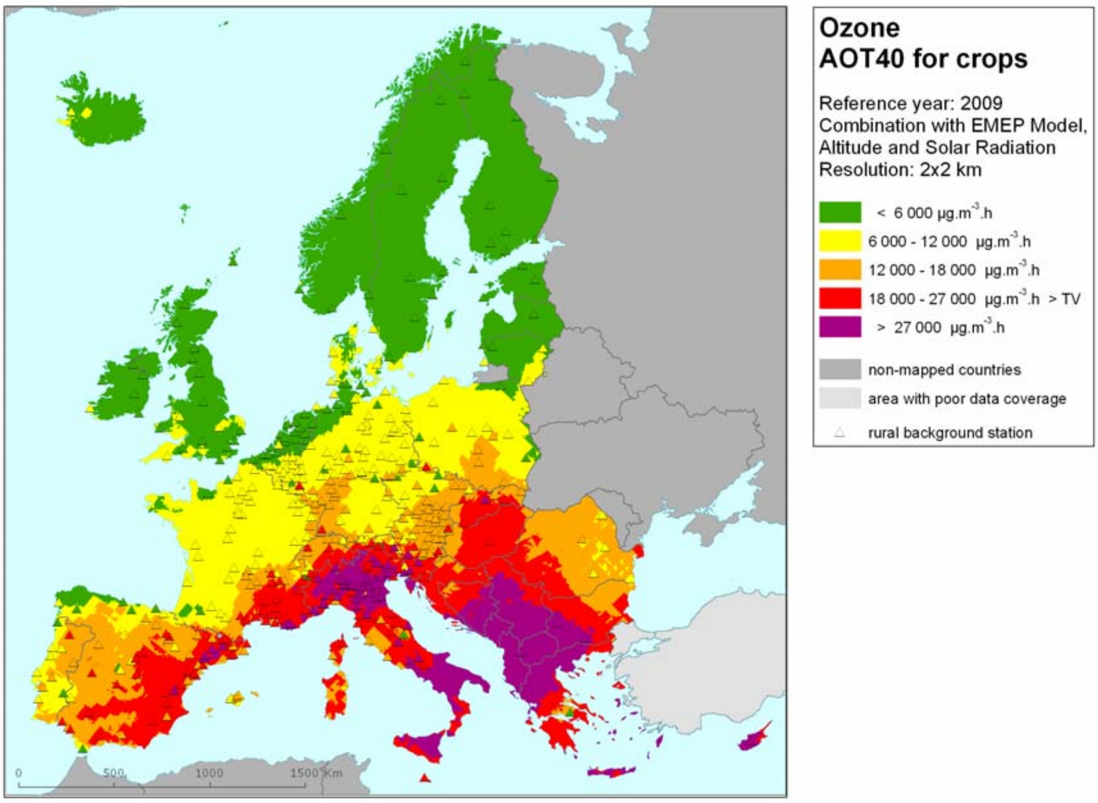

Figure 5.6 Rural concentration map of ozone vegetation indicator AOT40 for crops for the year 2009. Units: µg.m^{-3}.hours. Resolution: 2x2km.

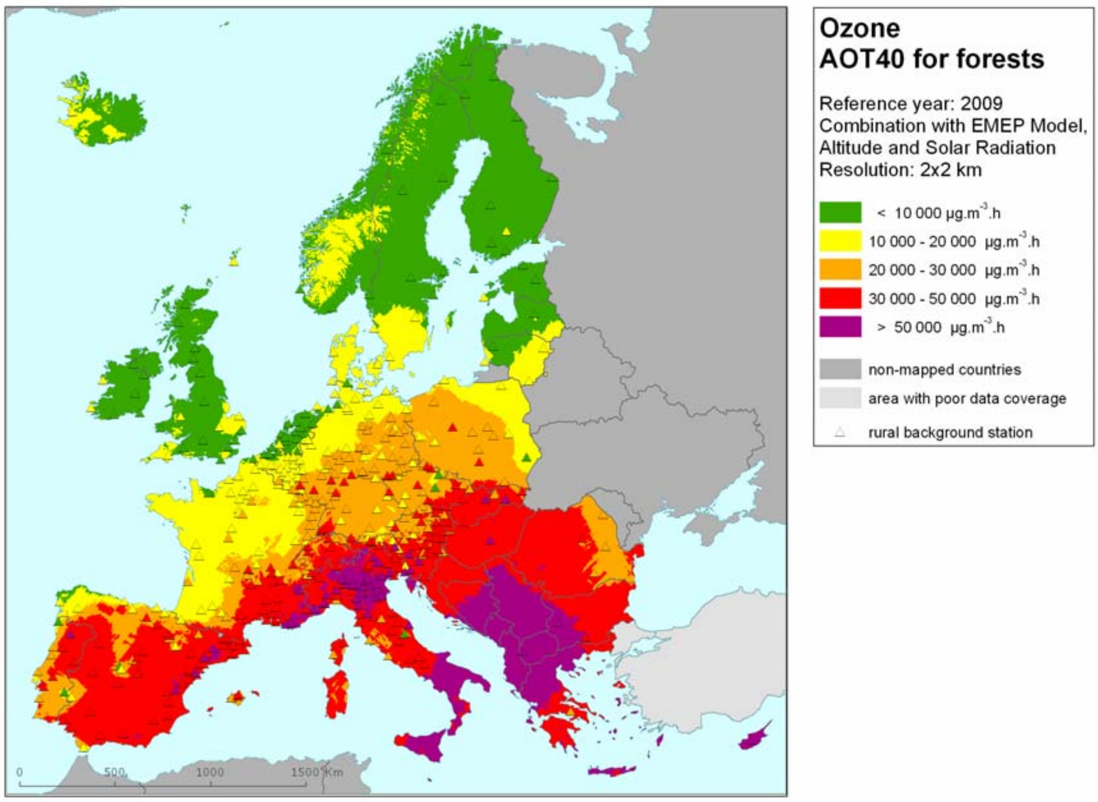

Figure 5.7 Rural concentration map of ozone vegetation indicator AOT40 for forests for the year 2009. Units: µg.m^{-3}.hours. Resolution: 2x2km.

Both maps show for 2009, compared to 2008 and 2007, specifically in the southern regions of Europe an increase in the extent of the areas with the highest AOT40 levels (red and purple). In the northern regions and in the northern-central part of Europe, the extent of the impacted areas is reduced in 2009 compared to 2008 and 2007.

5.3.2 Vegetation exposure

Agricultural crops

The rural map with ozone indicator AOT40 for vegetation, i.e. agricultural crops, as given in Figure 5.6 has been combined with the land cover CLC2000 map. Following a similar procedure as described in Horálek et al. (2007) the exposure of agricultural areas, defined as the Corine Land Cover level-1 class *2 Agricultural areas* (encompassing the level-2 classes *2.1 Arable land, 2.2 Permanent crops, 2.3 Pastures* and *2.4 Heterogeneous agricultural areas)* has been calculated at the country-level.

Table 5.8 gives the absolute and relative agricultural area for each country and for four European regions where the target value (TV) and long-term objective (LTO) for ozone are exceeded. The frequency distribution of the agricultural area per country over the exposure classes is presented as well.

The table indicates the country grouping with corresponding colours of the region; *Northern Europe*: Sweden, Finland, Norway, Estonia, Lithuania, Latvia and Denmark. *North-western Europe*: United Kingdom, Ireland, Iceland, the Netherlands, Belgium, Luxembourg and France north of 45 degrees latitude. *Central and Eastern Europe*: Germany, Poland, Czech Republic, Slovakia, Hungary, Austria, Liechtenstein, Bulgaria and Romania. *Southern Europe*: Albania, Bosnia-Herzegovina, France south of 45 degrees latitude, Portugal, Spain, Italy, San Marino, Slovenia, Croatia, Greece, Cyprus, F.Y.R. of Macedonia, Montenegro, Serbia and Malta.

Table 5.8 illustrates that in 2009 some 26 % of all European agricultural land was exposed to ozone exceeding the target value (TV) of 18 $mg.m^{-3}.h$ and 81 % was exposed to levels in excess of the long-term objective (LTO) of 6 $mg.m^{-3}.h$. This is a reduction in the total area with agricultural crops above the TV (and as such considered to suffer from adverse effects to ozone exposure) compared to 2008 (38 %), 2007 (36 %), and well below that of 2006 (70 %) and 2005 (49 %). Considering the long-term objective (LTO) the area in excess decreased to levels below 2008 (96 %), 2006 (98 %) and 2005 (89 %), but close to 2007 (78 %). Contrary to 2008, in 2009 some European countries did have ozone levels not being in excess of the LTO: mainly Scandinavian countries. In many countries of central and southern Europe, more than half of their total agricultural area experienced exposures above the target value as least stringent threshold.

In southern Europe, about 60 % of the total agricultural area exceeded in 2009 the target value. This is in within the range of what it was in 2008 (64 %) and 2007 (55 %), and substantially below the amounts of 2006 (94 %) and 2005 (96 %). In 2009, 2008, 2007 and 2005 no area is mapped in excess of the target value in northern Europe; only in 2006 about 4 % of its area was in excess of the target value. In the north-western region the area exceeding the target value is almost 50 % in 2006, which is more than four times larger than in 2005 (11 %). However, in the period 2009 – 2007 ozone levels have dropped such that only 0.1 – 2 % of the area was still in excess. For the central and eastern region, the total area where ozone exceeds the target value increased considerably from 2005 to 2006: from 44 % to 77 %. In 2007, it drops to an area of 50 % and in 2008 it further reduced to 47 % of the total area, being just above the level of 2005. In 2009, a further drop resulted in an area in exceedance of 17 %.

Compared to 2005, the frequency distribution of agricultural area over the exposure classes shows for 2006 a clear shift towards higher exposures leading to an increased total area exceeded. In 2007, this shift diminishes again to a distribution more similar to that of 2005, with a small increase in the area not exceeding the target value. In 2008, this tendency continues with about a similar area percentage in excess of the TV, however, including a shift in area percentages with lower exposure levels in 2007 to somewhat higher levels in 2008, but still below the target value. Compared to 2007 – 2008, we observed in 2009 an increased area with lower exposure level, leading to a lower TV exceedance.

Table 5.8 Agricultural area exposure and exceedance (Long Term Objective, LTO, and Target Value, TV) for ozone, AOT40 for crops, year 2009.

Country	Agricultural Area, 2009					Percentage of agricultural area, 2009 [%]				
	tot. area	> LTO (6 $mg.m^{-3}.h$)		> TV (18 $mg.m^{-3}.h$)		< 6 $mg.m^{-3}.h$	6 - 12 $mg.m^{-3}.h$	12 - 18 $mg.m^{-3}.h$	18 - 27 $mg.m^{-3}.h$	> 27 $mg.m^{-3}.h$
	[km^2]	[km^2]	[%]	[km^2]	[%]					
Albania	7178	7178	100	7178	100	0	0	0	0	100
Austria	27467	27467	100	1104	4.0	0	21.0	75.0	4.0	0.0
Belgium	17641	12355	70.0	0	0	30.0	70.0	0	0	0
Bosnia-Herzegovina	19300	19300	100	17428	90.3	0	0	9.7	50.1	40.2
Bulgaria	57364	57364	100	36954	64.4	0	0.6	35.0	49.7	14.8
Croatia	24096	24096	100	20605	85.5	0	0	14.5	75.6	9.9
Cyprus	4291	4291	100	4291	100	0	0	0.0	28.5	71.5
Czech Republic	45516	45516	100	0	0.0	0	66.5	33.5	0.0	0
Denmark (w~out Faroes)	32042	20756	64.8	0	0	35.2	64.8	0.0	0	0
Estonia	14678	2	0.0	0	0	100.0	0.0	0	0	0
Finland	28824	4	0.0	0	0	100.0	0.0	0	0	0
France	328377	328362	100.0	33446	10.2	0.0	62.0	27.8	10.2	0.0
Germany	213380	187786	88.0	0	0	12.0	77.9	10.1	0	0
Greece	51332	51332	100	48872	95.2	0	0	4.8	47.1	48.2
Hungary	63115	63115	100	52765	83.6	0	0	16.4	83.6	0
Iceland	2336	34	1.5	0	0	98.5	1.5	0	0	0
Ireland	46229	249	0.5	0	0	99.5	0.5	0	0	0
Italy	155409	155409	100	141779	91.2	0	0.1	8.7	37.9	53.3
Latvia	28273	4	0.0	0	0	100.0	0.0	0	0	0
Liechtenstein	44	44	100	0.0	0	0	0	100	0	0
Lithuania	40034	6545	16.3	0	0	83.7	16.3	0.0	0	0
Luxembourg	1410	1410	100	0	0	0	92.9	7.1	0	0
Macedonia	9511	9511	100	9511	100	0	0	0	0	100
Malta	122	122	100	122	100	0	0	0	100	0
Monaco	0.50	0.50	100	0.5	100	0	0	0	100	0
Montenegro	2398	2398	100	2398	100	0	0	0	0	100
Netherlands	24847	1659	6.7	0	0	93.3	6.7	0	0	0
Norway	15610	52	0.3	0	0	99.7	0.3	0	0	0
Poland	200526	187611	93.6	0	0.0	6.4	79.0	14.6	0.0	0
Portugal	42524	42250	99.4	0	0	0.6	57.1	42.3	0	0
Romania	134848	134848	100	28946	21.5	0	6.5	72.1	21.5	0
San Marino	42	42	100	42	100	0	0	0	100	0
Serbia (incl. Kosovo)	48510	48510	100	48510	100	0	0	0	38.6	61.4
Slovakia	24317	24317	100	14205	58.4	0	0	41.6	58.4	0.0
Slovenia	7126	7126	100	5209	73.1	0	0	26.9	70.7	2.4
Spain	252224	243557	96.6	88599	35.1	3.4	9.3	52.1	34.6	0.5
Sweden	38566	3802	9.9	0	0	90.1	9.9	0	0	0
Switzerland	11790	11790	100	1176	10.0	0	2.9	87.2	9.6	0.4
United Kingdom	141588	21269	15.0	0	0	85.0	15.0	0	0	0
Total	**2162885**	**1751482**	**81.0**	**563141**	**26.0**	**19.0**	**31.9**	**23.1**	**17.7**	**8.3**
France N of 45N	260636	260621	100.0	9895	3.8	0.0	70.1	26.1	3.8	0
France S of 45N	67741	67741	100	23551	34.8	0	30.6	34.6	34.8	0.0
Northern	198027	31164	15.7	0	0					
North-western	494687	297597	60.2	9895	2.0					
Central & eastern	778368	739858	95	135150	17.4					
Southern	691804	682863	98.7	418095	60.4					
Total	**2162885**	**1751482**	**81.0**	**563141**	**26.0**					

Note: Countries not included due to lack of land cover data: Andorra, Turkey.

Forests

The rural map with ozone indicator AOT40 for forests, as given in Figure 5.7 was combined with the land cover CLC2000 map as well. Following a similar procedure as described in Horálek et al. (2007) the exposure of forest areas, defined as the Corine Land Cover level-2 class *3.1. Forests,* has been calculated at the country-level.

Table 5.9 gives for each country, four European regions and Europe as a whole, the absolute and relative forest area where the *Reporting Value* (RV of 20 mg.m^{-3}.h, as Annex III of the ozone directive defines it) in combination with the *Critical Level* (*CL* of 10 mg.m^{-3}.h, as defined in the UNECE Mapping Manual) are exceeded. The table presents the frequency distribution of the forest area per country over the exposure classes as well. The Reporting Value of the ozone directive (RV) of 20 mg.m^{-3}.h is exceeded in 2009 at 49 % of the total European forest area, which is about the same as in 2008 (50 %) and 2007 (48 %), while in 2006 it was almost 70 % and in 2005 about 60 %. This means that the area of forest exposed to levels above the accumulated ozone Reporting Value initially increased in 2006 with 10 % and than diminished again in 2007 – 2009 to a smaller area of 10 % below that of 2005.

In 2005 three-quarters of the European forest areas were exposed to exceedances of the Critical Level of 10 mg.m^{-3}.h. In 2006 in about all forest areas, the Critical Level was exceeded. This shrank in 2007 to 62 %, but in 2008 it increased to 80 %. In 2009, the forest area exposed to exceedances was reduced to a level of 67 %.

All European countries had forests exposed to accumulated ozone concentrations above the Critical Level, while for most even all their forests suffered in 2009 exposures also in excess of the less stringent Reporting Value. Finland, Sweden, Norway, Iceland, Ireland, The Netherlands and the UK continued to show in 2009 accumulated ozone levels over forests not exceeding the reporting value and a further reduced part of their forests exceeding the Critical Level. In 2009, the list of countries without area above the RV but with CL exceedances was extended by Ireland, Latvia, Lithuania, Belgium and Estonia, with the last two countries showing almost all their forest areas exposed to levels above the CL.

As in previous years, in 2009 the southern European region had AOT40 levels where about all forested areas where exposed to exceedances of the Critical Level.

The central and eastern regions show for the period of 2009 – 2005 a continued 100 % exceedance of the Critical Levels. The area with exceedances of the Reporting Value showed a peak of 100 % in 2006, followed by a reduction to about 85 % in 2007, and a subsequent increase of about 10 % in 2008 to 94 %, which comes close to the 96 % of 2005. In 2009, the area in excess of the RV is 88 %. In the north-western region, the area exceeding the Critical Level increased from 84 % in 2005 to practically the whole area (98 %) in 2006. In 2007, it dropped again to 78 %, but in 2008 it increased to almost all forested area (94 %). In 2009, it is 81 %, close to the excess of 2007. Concerning the northwestern European forested area above the Reporting Value there was an increase observed from 69 % in 2005 to 80 % in 2006, with a prominent drop in 2007 to 28% that continued in 2008 to 24 %, but increased in 2009 to 30 %, being close to the value of 2007. Specifically in the northern region of Europe, the area in exceedance peaked considerably in 2006: the area above the Critical Level enlarged from 40 % in 2005 to 100 % in 2006 and reduced thereafter to 12 % in 2007 and increased in 2008 to 51 %. In 2009, some 23 % of the northern European forest area exceeded the CL. The Reporting Value peaks from no exceedance in 2005 to 23 % in 2006 back to none in 2007 – 2009. In comparison with 2005, the frequency distribution of the whole European forested area over the exposure classes shows for 2006 a clear shift to higher exposures, specifically for the areas which had the lowest class values and values well above the Reporting Value in 2005. In 2007 an opposite shift occurred to the lower neighbouring classes and for a more extended area than in 2005. In 2008 a shift was observed of areas exposed in 2007 to the highest exposures to its neighbouring lower class interval and for the areas exposed in 2007 to the lowest exposure class to its neighbouring higher class interval. In 2009 the distribution showed similarity with that of 2007. The total area with AOT40 levels below the Critical Level diminished by 18 % in 2008 (20 %) compared to 2007 (38 %) but increased again in 2009 up to

33 %; the total forested area submitted to levels below the Reporting Value stabilised in the period 2009 – 2007 around a value of 50 %.

Table 5.9 Forest area exposure and exceedance (critical level, CL, and reporting value, RV) for ozone, AOT40 for forests, year 2009.

Country	Area of forests, 2009					Percentage of forest area, 2009 [%]				
	tot. area	> CL (10 mg.m^{-3}.h)		> RV (20 mg.m^{-3}.h)		< 10	10 - 20	20 - 30	30 - 50	> 50
	[km^2]	[km^2]	[%]	[km^2]	[%]	mg.m^{-3}.h	mg.m^{-3}.h	mg.m^{-3}.h	mg.m^{-3}.h	mg.m^{-3}.h
Albania	7818	7818	100	7818	100	0	0	0	97.4	2.6
Austria	37613	37613	100	37613	100	0	0	47.3	52.7	0
Belgium	6090	6029	99.0	0	0	1.0	99.0	0	0	0
Bosnia-Herzegovina	22952	22952	100	22952	100	0	0	0.8	99.1	0.0
Bulgaria	34821	34821	100	34821	100	0	0	19.6	80.4	0
Croatia	20140	20140	100	20140	100	0	0	1.2	98.8	0
Cyprus	1551	1551	100	1551	100	0	0	26.5	73.5	0
Czech Republic	25455	25455	100	25455	100	0	0	57.6	42.4	0
Denmark	3641	3641	100	61	1.7	0	98.3	1.7	0	0
Estonia	20767	20687	99.6	0	0	0.4	99.6	0	0	0
Finland	193292	46061	23.8	0	0	76.2	23.8	0	0	0
France	144833	144719	99.9	75625	52.2	0.1	47.7	25.6	23.0	3.6
Germany	103821	103754	99.9	84086	81.0	0.1	18.9	77.7	3.3	0
Greece	23538	23538	100	23538	100	0	0	0	38.7	61.3
Hungary	17341	17341	100	17341	100	0	0	0	99.1	0.9
Iceland	314	53	16.9	0	0	83.1	16.9	0	0	0
Ireland	2906	12	0.4	0	0	99.6	0.4	0	0	0
Italy	78782	78782	100	78782	100	0	0	2.1	65.0	32.8
Latvia	26915	3257	12.1	0	0	87.9	12.1	0	0	0
Liechtenstein	66	66	100	66	100	0	0	40.5	59.5	0
Lithuania	18659	12041	65	0	0	35	65	0	0	0
Luxembourg	908	908	100	908	100.0	0	0	100	0	0
Macedonia, FYR	8641	8641	100	8641	100	0	0	0	0	100
Malta	2	2	100	2	100	0	0	0	0	100
Monaco	1	1	100	1	100	0	0	0	13.1	86.9
Montenegro	5776	5776	100	5776	100	0	0	0	0	100
Netherlands	3101	893	28.8	0	0	71.2	28.8	0	0	0
Norway	104755	15815	15.1	0	0.0	84.9	15.1	0	0	0
Poland	91804	91804	100	64222	70.0	0	30.0	66.0	3.9	0
Portugal	24299	24299	100	23255	95.7	0	4.3	51.8	43.9	0
Romania	69775	69775	100	69775	100.0	0	0	13.3	86.0	1
San Marino	7	7	100	7	100	0	0	0	100	0
Serbia (incl. Kosovo)	26706	26706	100	26706	100	0	0	0	7.9	92.1
Slovakia	19322	19322	100	19322	100	0	0	6.4	93.6	0
Slovenia	11486	11486	100	11486	100	0	0	0	97.7	2.3
Spain	91844	89052	97.0	81155	88.4	3.0	8.6	18.7	68.1	1.5
Sweden	249830	42617	17.1	0	0	82.9	17.1	0	0	0
Switzerland	12504	12504	100	12497	100	0	0.1	29.4	67.5	3.0
United Kingdom	19617	1986	10.1	0	0	89.9	10.1	0	0	0
Total	**1531692**	**1031923**	**67.4**	**753599**	**49.2**	**32.6**	**18.2**	**17.3**	**26.2**	**5.7**
France N of 45N	89507	89394	99.9	35698	39.9	0.1	60.0	32.5	7.4	0.1
France S of 45N	55326	55326	100	39927	72.2	0	27.8	14.5	48.3	9.4
Northern	617859	144119	23.3	61	0.0					
North-western	122445	99275	81.1	36606	29.9					
Central & eastern	412521	412454	100.0	365197	88.5					
Southern	378867	376075	99.3	351735	92.8					
Total	**1531692**	**1031923**	**67.4**	**753599**	**49.2**					

Note: Countries not included due to lack of land cover data: Andorra, Turkey.

5.3.3 Uncertainties

Uncertainty estimated by cross-validation

In Table 5.7 the absolute mean uncertainty (RMSE) obtained by cross-validation is 5138 µg.m^{-3}.h for the AOT40 for crops and 9311 µg.m^{-3}.h for the AOT40 for forests. It indicates that the year 2009 has lower absolute mean uncertainties for the crops than in previous years: 5283 µg.m^{-3}.h (2008), 5876 µg.m^{-3}.h (2007), 7674 µg.m^{-3}.h (2006) and 7700 µg.m^{-3}.h (2005). For forests it is slightly higher than the value 8750 µg.m^{-3}.h in 2008, but still well below those of 2007 (10190 µg.m^{-3}.h), 2006 (11990 µg.m^{-3}.h) and 2005 (12500 µg.m^{-3}.h). The relative mean uncertainty of the 2009 map of ozone indicator AOT40 for crops is about 38% and of the map of AOT40 for forests about 34 %. For crops that is of similar level as in 2007 (40 %) and 2005 (41 %), but higher than in 2008 (31 %) and 2006 (30%). For forests it is the same is in 2008 and 2006, and lower than in 2007 (37 %) and 2005 (41%). From these values, one cannot conclude on a certain tendency.

Figure 5.9 shows the cross-validation scatter plots of the AOT40 for both crops and forests. R^2 indicates that for AOT40 for crops about 69 % and for AOT40 for forests about 68 % of the variability is attributable to the interpolation. The corresponding values for the 2008 maps (53 % and 56 %), 2007 maps (63 % and 67 %), the 2006 maps (47 % and 49 %) and 2005 maps (55 % and 58 %), indicates a somewhat increased level of interpolation performance at the 2009 maps compared to those of previous years.

The cross-validation scatter plots show again that in areas with higher accumulated ozone concentrations the interpolation methods tend to deliver underestimated predicted values. For example, in agricultural areas (Figure 5.9, left panel) an observed value of 30 000 µg.m^{-3}.h is estimated in the interpolation as about 25 300 µg.m^{-3}.h, i.e. an underestimation of about 16 %. In addition, an overestimation at the lower end of predicted values occurred. One could reduce this under- and overestimation by extending the number of measurement stations and by optimising the spatial distribution of those stations, specifically in areas with elevated values.

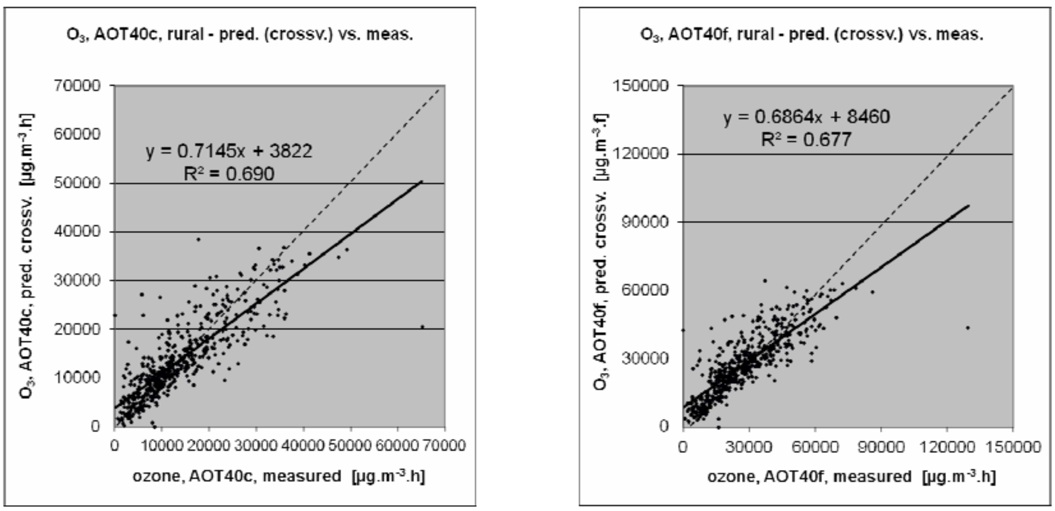

Figure 5.9 Correlation between cross-validation predicted values (y-axis) and measurements (x-axis) for the ozone indicators AOT40 for crops (left) and AOT40 for forests (right) for rural areas in 2009.

Comparison of point measurement values with the predicted grid value

Additional to the point observation - point prediction cross-validation, a simple comparison was made between the point measurements and interpolated predicted grid values averaged in a 2 x 2 km^2 grid.

The results of the cross-validation compared to the gridded validation are summarised in Table 5.10. The table shows for both receptors a better correlation between the station measurements and the averaged interpolated predicted values of the corresponding grid cells (case ii) than it does at the point cross-validation predictions (case i) of Figure 5.9. Case ii) represents the uncertainty in the predicted gridded interpolation map at the actual station locations (points) itself, whereas the point observation – point prediction cross-validation of case i) simulates the behaviour of the interpolation at point positions without actual measurements within the area covered by measurements. The uncertainty at measurement locations has partly its cause in the smoothing effect of interpolation and partly in the spatial averaging of the values in the 2 x 2 km^2 grid cells. The level of the smoothing effect leading to underestimation at areas with high values is there smaller than it is in case no measurement is present in such areas. For example, in agricultural areas the predicted interpolation grid value will be about 27 000 µg.m^{-3}.h at the corresponding station point with the observed value of 30 000 µg.m^{-3}.h, i.e. an underestimation of about 10 %.

Table 5.10 Linear regression equation and coefficient of determination R^2 from the scatter plots of (i) the predicted point values based on cross-validation and (ii) aggregation into 2x2 km grid cells versus the measured point values for PM_{10} indicator annual average for rural (left) and urban (right) areas of 2009.

	AOT40 for crops		**AOT40 for forests**	
	equation	**R^2**	**equation**	**R^2**
i) cross-validation prediction (Fig 5.9)	y = 0.715x + 3822	0.690	y = 0.686x + 8460	0.677
ii) 2x2 km grid prediction	y = 0.823x + 2388	0.875	y = 0.814x + 5053	0.881

The AOT40 for crops with a target value of 18 000 µg.m^{-3}.h would allow us to prepare a probability of exceedance map. However, we limited the preparation of such maps to the human health related indicators, thus not involving the accumulative ozone indicators used in the EEA CSI005, not demanding such maps.

6 Concluding exposure and uncertainty estimates

Mapping and exposure results

This paper presents the interpolated maps for 2009 on the PM_{10} and ozone human health related air pollution indicators, together with their frequency distribution of the estimated population exposures and exceedances. It concerns the annual average and the 36th maximum daily mean for PM_{10} and the SOMO35 for ozone. Additionally, presented are for ozone the interpolated maps on the vegetation/ecosystem based indicators AOT40 for crops and AOT40 for forests, including their frequency distribution of estimated land area exposures and exceedances. A similar mapping approach, primarily based on station observational data, has been used as in previous years (De Smet et al. (2011) and references cited therein).

Human health PM_{10} indicators

Table 6.1 summarises for both *human health PM_{10} indicators* the average concentration the European inhabitant is exposed to, i.e. the population-weighted concentration, and the number of Europeans exposed to PM_{10} concentrations above their limit values (LV) for the years 2005 to 2009. The table presents the results obtained with the merging resolution on both the 10x10 km^2 grid, as used at previous data years up to 2007, and the 1x1 km^2 grid as tested with the 2006 data in Horálek et al (2010) and implemented fully on the 2008 data and onwards. It provides an indication that the underestimation of PM10 values at merging with the 10x10 km^2 grid resolution has been resolved better when using a higher 1x1 km^2 grid resolution. In other words, an increased merging resolution contributes to a quantitatively better population exposure estimate due to better resolving the spatially smaller urbanised patterns in the map.

Table 6.1 Percentage of the total European population exposed to PM_{10} concentrations above the limit values (LV) and the population-weighted concentration for the human health PM_{10} indicators annual average and 36th maximum daily average for 2005 to 2009.

PM10			2005	2006	2007	2008	2009
Annual average							
Population-weighted concentration	(µg.m^{-3})	10x10 merger	26.3	27.1	25.3		
		1x1 merger		28.5		24.8	24.6
Population exposed > LV (40 µg.m^{-3})	(% of total)	10x10 merger	9.3	7.7	5.7		
		1x1 merger		9.8		5.8	6.0
36th max. daily average							
Population-weighted concentration	(µg.m^{-3})	10x10 merger	43.8	45.4	42.4		
		1x1 merger		47.8		41.3	41.2
Population exposed > LV (50 µg.m^{-3})	(% of total)	10x10 merger	28.1	28.5	22.0		
		1x1 merger		35.7		19.4	16.5

The population exposed to *annual mean* concentrations of PM_{10} above the limit value of 40 µg.m^{-3} is at least 6 % of the total population in 2009 and similar to that of 2008. Furthermore, it is estimated that the European inhabitants living in the background (neither hot-spot nor industrial) areas – without regard to urban or rural – are, as in 2008, exposed on average to the annual mean PM_{10} concentration of almost 25 µg.m^{-3}. In comparison with the previous three years, the number of people living in the areas above the LV originally tends to go down slightly. It is not possible to talk about a trend when taking into account (i) the increased merging resolution applied on the 2008 data for the first time, (ii) the meteorologically induced variations and (iii) the uncertainties involved in the interpolation. Longer time series and reduced uncertainties will be needed before drawing any conclusions on a possible trend.

In 2009 at least 16 % of the European population lived in areas where the PM_{10} limit value of 50 µg.m^{-3} for the *36th maximum daily mean* is exceeded, being some 3 % lower than in 2008, 2-3 % lower than in 2007 and 8-9 % lower than in 2006 and 2005. The overall European population-weighted concentration of the 36th maximum daily mean for the background areas is estimated at about 41 µg.m^{-3}, which is the same as in 2008. Compared to the preceding years 2007 – 2005, one cannot simply conclude on some tendency, except that in 2009 – 2007 the highest daily averages had lower concentrations than in 2006 and 2005, probably leading to a population exposed to slightly lower concentrations. Increased merging resolution was applied to the 2008 and 2009 data. That by itself leads to an increased number of the population exposure. Comparing the observed exceedances for both PM_{10} indicators, one can conclude that the daily limit value is the most stringent throughout the years.

Human health ozone indicators

Table 6.2 summarises for both *human health ozone indicators* the average concentration the European inhabitants are exposed to, i.e. the population-weighted concentration. Furthermore, the number of Europeans exposed to concentrations above the limit values (LV) of the 26th highest daily maximum 8-hour mean and above a level of 6 mg.m^{-3}.d for the SOMO35 for the years 2005 to 2009 is presented. The table presents the results obtained with the merging resolution on both the 10x10 km^2 grid, as used at previous data years up to 2007, and the 1x1 km^2 grid as tested on the 2006 data in Horálek et al (2010) and implemented fully on the 2008 data and onwards. It provides an indication that the overestimation of ozone values at merging with the 10x10 km^2 grid resolution has been resolved better when using a higher 1x1 km^2 grid resolution. In other words, an increased merging resolution contributes to a quantitatively better population exposure estimate due to better resolving the spatially smaller urbanised patterns in the map.

Table 6.2 Percentage of the total European population exposed to ozone concentrations above the target value (TV) for the 26th highest daily maximum 8-hour average and an indicative chosen threshold for SOMO35, including their population-weighted concentrations for2005 to 2009.

Ozone			2005	2006	2007	2008	2009
26th highest daily max. 8-hr average							
Population-weighted concentration	(µg.m^{-3})	10x10 merger	112.9	119.6	112.1		
		1x1 merger		118.2		109.8	108.1
Population exposed > TV (120 mg.m^{-3}.h)	(% of total)	10x10 merger	37.8	55.5	33.5		
		1x1 merger		51.4		15.0	16.0
SOMO35							
Population-weighted concentration	(µg.m^{-3})	10x10 merger	5047	5485	4679		
		1x1 merger		5167		4275	4275
Population exposed > 6 mg.m^{-3}.d	(% of total)	10x10 merger	33.9	37.4	32.6		
		1x1 merger		29.5		19.6	24.6

For the ozone indicator *26th highest daily maximum 8-hour mean* it is estimated that at least 16 % of the population lived in 2009 in areas above the ozone target value (TV) of 120 µg.m^{-3}, which was similar to that of 2008. The overall European population-weighted ozone concentration in terms of the 26th highest daily maximum 8-hour mean in the background areas is estimated at almost 108 µg.m^{-3} and close to that of 2008 (110 µg.m^{-3}). Compared to the previous years 2005 – 2007, one could conclude that 2006 is a year with elevated ozone concentrations, leading to increased exposure levels compared to the other four years. Additionally, the population exposed to ozone level above the target value is in 2009 – 2008 substantially lower than in the preceding period 2007 – 2005. The increased merging resolution will have partially caused the reduced value in the last two years.

Similar tendency is observed for the *SOMO35*: in 2005 and 2007 one-third of the population lived in areas where a level of 6 mg.m^{-3}.d$^{(*)}$ was exceeded and being slightly lower than the estimated 37 % in 2006. In 2008 it concerns only one-fifth of the population, and a quarter of it in 2009. The population weighted SOMO35 concentrations shows a similar pattern in time. The increase of 2006 occurs specifically in areas of northern and north-western Europe where the lowest SOMO35 levels are found. In 2008 and 2009 however, these reduced levels did appear less prominently.

(*) Note that the 6 mg.m^{-3}.d does not represent a legally binding 'threshold'. In this and previous papers it concerns a somewhat arbitrarily chosen threshold to facilitate the discussion of the observed distributions of SOMO35 levels in their spatial and temporal context. This choice is based on a comparison of the 26th highest daily max. 8-hour means versus the SOMO35 of the ozone concentration measurements at all background stations in The Netherlands. The SOMO35 is estimated to be about 4 mg.m^{-3}.d when no Dutch population is exposed to ozone concentrations above the target value of the 26th h.d.m.8-hour mean. The Netherlands has in general relative low ozone concentrations compared to most other European countries. Over the years we applied the level of 6 mg.m^{-3}.d in our discussions of the annual results for two reasons: (i) to compensate for a possible underestimation of the SOMO35, and (ii) to match with a class interval limit of the SOMO35 map (Figure 5.4).

Agricultural and forest ozone indicators

Exposure indicators describing the *agricultural and forest areas exposed to accumulated ozone* concentrations above defined thresholds are summarised in Table 6.3. They are the target value (LV) of 18 mg.m^{-3}.h and the long-term objective (LTO) of 6 mg.m^{-3}.h for the AOT40 for crops, and the Reporting Value (RV) of 20 mg.m^{-3}.h and the Critical Level (CL) of 10 mg.m^{-3}.h for the AOT40 for forests.

Table 6.3 Percentages of the total European agricultural and forest area exposed to ozone concentrations above their thresholds: target value (TV) and long-term objective (LTO) for AOT40 for crops, and Critical Level (CL) and Reporting Value (RV) for AOT40 for forests for2005 to 2009.

Ozone		2005	2006	2007	2008	2009
AOT40 for crops						
Agricultural area % > TV (18 mg.m^{-3}.h)	(% of total)	48.5	69.1	35.7	37.8	26.0
Agricultural area % > LTO (6 mg.m^{-3}.h)	(% of total)	88.8	97.6	77.5	95.5	81.0
AOT40 for forests						
Forest area exposed > RV (20 mg.m^{-3}.h)	(% of total)	59.1	69.4	48.4	50.2	49.2
Forest area exposed > CL (10 mg.m^{-3}.h)	(% of total)	76.4	99.8	62.1	79.6	67.4

In 2009, 26 % of all agricultural land (*crops*) was exposed to accumulated ozone concentrations exceeding the target value (TV) and 81 % was exposed to levels in excess of the long-term objective (LTO). Compared to the previous four years one could conclude that 2006 was a year with elevated ozone concentrations, leading to increased exposure levels above the target value and that they subsided in the period 2007 – 2009 to levels clearly below those of 2005. On the other hand, the percentage of the total area exposed to levels above the long-term objective (LTO) is in 2007 lowest compared to all the other years.

For the ozone indicator AOT40 for *forests* the level of 20 mg.m^{-3}.h (RV) was in 2009 exceeded in almost half of the European forest area, which is similar to 2008 and 2007 and clearly below the percentages of the years 2005 and 2006. The forest area exceeding the Critical Level was in 2009 about two-thirds, which is somewhat more than in 2007 (62 %), but well below 2008 and 2005 with 76 – 80 % exceedance, and 2006- when all forest area was exceeded.

The temporal pattern of the AOT40 for forests exceedances shows some similarity with those of the AOT40 for crops, despite their different definitions. This annual variability is heavily dependent on meteorological variability.

The results in this report show that in general over Europe and most significantly over northern and north-western Europe, 2006 was characterised by higher ozone levels than in 2005 and 2007 – 2009: all indicators show an increase in 2006.

Uncertainty results

Next to the creation of European wide interpolated air pollutant maps and exposure tables, we evaluated the uncertainty of the presented concentration maps and maps with estimated probability of threshold exceedance for the human health indicators. As exactly the same method and data sources have been applied over the years 2005 to 2009 a change in uncertainty is in principle related to the data content itself,. However, for the 2008 data we implemented for the first time an increased resolution (from a 10x10 km^2 into 1x1 km^2 grid field) at the merging of the separate human health indicator interpolated maps (on 10x10 km^2 grid) into one combined final 1x1 km^2 gridded indicator map. The merging made use of the 1x1 km^2 population density map. (The subsequent exposure estimates however, have been based on the 10x10 km^2 grid fields, aggregated from the 1x1 km^2 grids of the merging result). The increased merging resolution should in principle improve the accuracy in the concentration maps, and reduce the interpolation uncertainty of these maps, including the subsequent exposure estimates. Denby et al. (2008) discusses a diversity of uncertainty factors potentially involved, including their possible levels of influence. More background information on causes of uncertainties and their assessment can be found in Malherbe et al (2012). The paper recommends options to reduce uncertainties systematically. Horálek et al. (2010) explored specific options to reduce interpolation uncertainty related to the spatial resolutions applied at the different process steps of the mapping method. This paper concludes and justifies the implementation of the increased merging grid as the most significant uncertainty reduction measure, against the least additional computational demands.

Table 6.4 summarises the absolute and relative mean interpolation uncertainties of the PM_{10} maps for the four years sequence. The uncertainties in 2007 are slightly lower than in the other four years; this is probably given by the better fit of the linear regression with supplementary data in 2007 compared to the other years. For the rural areas, the absolute and relative uncertainties are the same as in 2007; for the urban areas, 2009 appears to have the highest absolute and relative uncertainty.

Table 6.4 Absolute mean uncertainty (RMSE, $\mu g.m^{-3}$) and relative mean uncertainty (RMSE relative to mean indicator value, in %) for the total European rural and urban areas for PM_{10} annual average and the 36th maximum daily average for the years 2005 – 2009.

PM10			2005	2006	2007	2008	2009
Annual average							
rural areas	abs. mean uncertainty	RMSE ($\mu g.m^{-3}$)	5.5	5.8	4.6	5.0	4.6
	rel. mean uncertianty	%	*25*	*27*	*24*	*27*	*24*
urban areas	abs. mean uncertainty	RMSE ($\mu g.m^{-3}$)	5.5	6.1	5.0	6.3	6.7
	rel. mean uncertianty	%	*20*	*21*	*18*	*22*	*23*
36th max. daily average							
rural areas	abs. mean uncertainty	RMSE ($\mu g.m^{-3}$)	9.8	13.3	8.0	8.8	8.0
	rel. mean uncertianty	%	*27*	*26*	*24*	*28*	*24*
urban areas	abs. mean uncertainty	RMSE ($\mu g.m^{-3}$)	11.7	9.9	9.1	12.7	13.2
	rel. mean uncertianty	%	*24*	*21*	*20*	*24*	*27*

The relative mean interpolation uncertainty of the ozone maps in Table 6.5 at the rural areas decreased slightly for the human health indicators in 2009, compared to previous years. The relative uncertainties of the health indicators for the urban areas increased in 2009 somewhat compared to previous years. In 2009, the vegetation-oriented AOT40 indicators showed in comparison with 2008 an increased relative uncertainty for the crops and the same value as in 2008 for the forests, whereas the absolute uncertainties increased for both vegetation types slightly compared to 2008. In cases where the absolute uncertainty increases and simultaneously the relative uncertainty decreases, the absolute mean of the indicator has increased relatively more than its absolute RMSE.

In general, one could conclude that the decrease in the absolute mean uncertainties in the period of 2005 – 2008 stopped in 2009.

Table 6.5 Absolute and relative mean uncertainty for the total European areas for ozone the 26th highest daily maximum 8-hour average, SOMO35, AOT40 for crops and for forests, for the years 2005 – 2009.

Ozone			**2005**	**2006**	**2007**	**2008**	**2009**
26th highest daily max. 8-hr average							
rural areas	abs. mean uncertainty	RMSE ($\mu g.m^{-3}$)	12.3	11.2	8.8	8.7	8.2
	rel. mean uncertianty	%	*10.3*	*8.9*	*7.5*	*7.6*	*7.2*
urban areas	abs. mean uncertainty	RMSE ($\mu g.m^{-3}$)	10.0	10.2	8.9	8.8	9.3
	rel. mean uncertianty	%	*8.9*	*8.4*	*7.9*	*7.9*	*8.4*
SOMO35							
rural areas	abs. mean uncertainty	RMSE ($\mu g.m^{-3}.d$)	2173	2077	1801	1609	1635
	rel. mean uncertianty	%	*35.5*	*31.6*	*33.3*	*30.7*	*29.7*
urban areas	abs. mean uncertainty	RMSE ($\mu g.m^{-3}.d$)	1459	1472	1260	1293	1475
	rel. mean uncertianty	%	*32.0*	*29.2*	*29.5*	*31.3*	*33.1*
AOT40 for crops							
rural areas	abs. mean uncertainty	RMSE ($\mu g.m^{-3}.h$)	7677	7674	5876	5283	5138
	rel. mean uncertianty	%	*40.7*	*29.6*	*39.6*	*31.3*	*37.7*
AOT40 for forests							
rural areas	abs. mean uncertainty	RMSE ($\mu g.m^{-3}.h$)	12474	11990	10190	8750	9311
	rel. mean uncertianty	%	*41.5*	*33.6*	*37.1*	*34.0*	*34.0*

The scatter plots of the interpolation results versus the measurements show that for both the PM_{10} and the ozone indicators in areas with high values, a underestimation of the predicted values occurs, leading also to a considerable underestimation at locations without measurements and at areas with the higher concentrations. This effect occurs most prominently for the ozone indicators. We expect that the underestimation would reduce when an improved fit of the linear regression with (other) supplementary data could be obtained. For example, in the near future more contributions from satellite imagery data and interpretation techniques could be expected. An option is to extend the number of measurement stations and/or using additional mobile stations (e.g. in measurement campaigns). Continued efforts aiming for a more optimised spatial distribution of (such) stations, especially in areas with high air pollution, and reduction of external uncertainties would likely contribute to reducing uncertainties in the interpolations. For further reading on this subject, we refer to Denby et al. (2009), Gerharz et al. (2011) and Gräler et al. (2012).

Probability of exceedance

Maps with the probability of exceedance of Limit Values and Target Value have been prepared for the human health indicators of PM_{10} and ozone, respectively. These probability maps, with a class distribution as defined in Table 4.4, are derived from combining the indicator map and its uncertainty map following the same method throughout the years 2005 to 2009. The differences in the maps between years depend on annual fluctuations in concentration levels, supplementary data and their involved uncertainties. (Denby et al. 2009), Gerharz et al. (2011) and Gräler et al. (2012). Some disruption or 'jump' could be expected between the data of 2005-2007 and 2008 – 2009. This would be caused by the increased merging resolution applied for the first time on the 2008 data. As Horálek et al. (2010) indicated, it should improve the interpolation accuracy and reduce the interpolation uncertainty, specifically for urban areas that profit most of this methodological refinement. However, the data in the tables of this paper do not show such a clear effect that it could be deduced from this fine-tuning of the mapping methodology. We assume in the first instance, however without proof, that this improvement is masked by the annual variability inherent to the data sources used in the regressions and interpolations. Especially the annual variability of the meteorological parameters would play a significant role.

In 2009 for the annual average $PM_{10,}$ the patterns in the spatial distribution of the different probability of exceedance (PoE) classes over Europe were similar to those of 2008. However, 2009 showed slightly higher values in the Po Valley and Torino area in Italy, Upper Silesia area in Poland, the area at Thessaloniki in Greece and the area of Sofia and Plovdiv in Bulgaria, albeit below the values of 2007 – 2005.

The 36th maximum daily means of PM_{10} do show until 2008, in general and throughout Europe, a reduction of both the extent of areas and the elevation of its levels of likelihood of exceedances. In 2009, however, there was a slight increase in the levels in areas with the higher PoE. In many areas, these reductions until 2008 consist of shifts to one lower PoE class, except at some of the kernels of agglomerations and industrial regions where elevated PoE continue to exist and subsequently increase in 2009 to higher probabilities of exceedance. In these areas, considerable emission reductions may still be needed to reach non-exceedance levels in the future.

Interpreting 2009 and its preceding four years, one can conclude for ozone that in 2006 the probability of exceedance (PoE) increased temporarily in most parts of Europe. In 2007 – 2009, Central Europe showed a continued decrease of PoE to levels, in many areas, well below those of 2005. Most areas with large PoE in 2007 showed in 2008 moderate and even modest levels of PoE that increased again somewhat in 2009. For 2009 similar and increased levels of likelihood of exceedance was estimated for the northern region of Italy, parts of Greece, the Balkan region, central-eastern European countries, the mountainous and urbanised areas of the Iberian Peninsula, the Alps and South-West Germany.

References

AirBase, European air quality database, http://airbase.eionet.europa.eu

Cressie N (1993). Statistics for spatial data. Wiley series, New York.

De Leeuw F, Horálek J (2009). Assessment of the health impacts of exposure to PM2.5 at a European level. ETC/ACC Technical Paper 2009/1. http://acm.eionet.europa.eu/reports/ETCACC_TP_2009_1_European_PM2.5_HIA

De Leeuw F, Ruyssenaars P (2011). Evaluation of current limit and target values as set in the EU Air Quality Directive. ETC/ACM Technical Paper 2011/3. http://acm.eionet.europa.eu/reports/ETCACM_TP_2011_3_evaluationAQ_LV_LT

Denby B, Horálek J, Walker SE, Eben K, Fiala J (2005). Interpolation and assimilation methods for European scale air quality assessment and mapping. Part I: Review and recommendations. ETC/ACC Technical paper 2005/7. http://acm.eionet.europa.eu/reports/ETCACC_TechnPaper_2005_7_spatial_AQ_interpol_Part_I

Denby B, Schaap M, Segers A, Builtjes P, Horálek J (2008). Comparison of two data assimilation methods for assessing PM_{10} exceedances on the European scale. Atmospheric Environment 42, 7122–7134.

Denby B, De Leeuw F, De Smet P, Horálek J (2009). Sources of uncertainty and their assessment in spatial mapping, ETC/ACC Technical Paper 2008/20. http://acm.eionet.europa.eu/reports/ETCACC_TP_2008_20_spatialAQ_uncertainties

Denby B, Gola G, De Leeuw F, De Smet P, Horálek J (2011a). Calculation of pseudo PM2.5 annual mean concentrations in Europe based on annual mean PM10 concentrations and other supplementary data. ETC/ACC Technical Paper 2010/9. http://acm.eionet.europa.eu/reports/ETCACC_TP_2010_9_pseudo_PM2.5_stations

Denby Rolstad B, Horálek J, de Smet P, de Leeuw F (2011b). Mapping annual mean $PM_{2.5}$ concentrations in Europe: application of pseudo $PM_{2.5}$ station data. ETC/ACM Technical Paper 2011/5. http://acm.eionet.europa.eu/reports/ETCACM_TP_2011_5_spatialPM2.5mapping

De Smet P, Horálek J, Coňková M, Kurfürst P, de Leeuw F, Denby B (2009). European air quality maps of ozone and PM10 for 2006 and their uncertainty analysis. ETC/ACC Technical Paper 2008/8. http://acm.eionet.europa.eu/reports/ETCACC_TP_2008_8_spatAQmaps_2006

De Smet P, Horálek J, Coňková M, Kurfürst P, de Leeuw F, Denby B (2010). European air quality maps of ozone and PM10 for 2007 and their uncertainty analysis. ETC/ACC Technical Paper 2009/9. http://acm.eionet.europa.eu/reports/ETCACC_TP_2009_9_spatAQmaps_2007

De Smet P, Horálek J, Coňková M, Kurfürst P, de Leeuw F, Denby B (2011). European air quality maps of ozone and PM10 for 2008 and their uncertainty analysis. ETC/ACC Technical Paper 2010/10. http://acm.eionet.europa.eu/reports/ETCACC_TP_2010_10_spatAQmaps_2008

EC (2008). Directive 2008/50/EC of the European Parliament and of the Council of 21 May 2008 on ambient air quality and cleaner air for Europe. OJ L 152, 11.06.2008, 1-44. http://eur-lex.europa.eu/LexUriServ/LexUriServ.do?uri=OJ:L:2008:152:0001:0044:EN:PDF

ECMWF: Meteorological Archival and Retrieval System (MARS). It is the main repository of meteorological data at ECMWF (European Centre for Medium-Range Weather Forecasts). http://www.ecmwf.int/

EEA (2011). Corine land cover 2000 (CLC2000) raster data. 100x100m gridded version 15 (08/2011). http://www.eea.europa.eu/data-and-maps/data/corine-land-cover-2000-raster-1

EEA (2008). ORNL Landscan 2008 Global Population Data conversion into EEA ETRS89-LAEA5210 1km grid resolution (eea_r_3035_1_km_landscan-eurmed_2008, by Hermann Peifer of EEA; contact person Paul Hasenohr, EEA).

Eurostat (2011). Total population for European states for 2009. http://epp.eurostat.ec.europa.eu/tgm/table.do?tab=table&language=en&pcode=tps00001&tableSelection=1&footnotes=yes&labeling=labels&plugin=1
Fagerli H, et al (2011). Transboundary acidification, eutrophication and ground level ozone in Europe in 2009. EMEP Report 1/2011. http://emep.int/publ/reports/2011/status_report_1_2011.pdf
Gerharz L, Gräler B, Pebesma E (2011). Measurement artefacts and inhomogeneity detection, ETC/ACM Technical Paper 2011/8. http://acm.eionet.europa.eu/reports/ETCACM_TP_2011_8_artefacts_inhom_detection
Gräler B, Gerharz L, Pebesma E (2012). Spatio-temporal analysis and interpolation of PM_{10} measurements in Europe, ETC/ACM Technical Paper 2011/10. http://acm.eionet.europa.eu/reports/ETCACM_TP_2011_10_spatio-temp_AQinterpolation
Horálek J, Kurfürst P, Denby B, de Smet P, de Leeuw F, Brabec M, Fiala J (2005). Interpolation and assimilation methods for European scale air quality assessment and mapping. Part II: Development and testing new methodologies. ETC/ACC Technical paper 2005/8. http://acm.eionet.europa.eu/docs/ETCACC_TechnPaper_2005_8_SpatAQ_Part_II.pdf
Horálek J, Denby B, de Smet PAM, de Leeuw FAAM, Kurfürst P, Swart R, van Noije T (2007). Spatial mapping of air quality for European scale assessment. ETC/ACC Technical paper 2006/6. http://acm.eionet.europa.eu/reports/ETCACC_TechnPaper_2006_6_Spat_AQ
Horálek J, de Smet PAM, de Leeuw FAAM, Denby B, Kurfürst P, Swart R, (2008). European air quality maps including uncertainty analysis. ETC/ACC Technical paper 2007/7. http://acm.eionet.europa.eu/reports/ETCACC_TP_2007_7_spatAQmaps_ann_interpol
Horálek J, de Smet PAM, de Leeuw FAAM, Coňková M, Denby B, Kurfürst P (2010). Methodological improvements on interpolating European air quality maps. ETC/ACC Technical Paper 2009/16. http://acm.eionet.europa.eu/reports/ETCACC_TP_2009_16_Improv_SpatAQmapping
Jimmink B, de Leeuw F, Ostatnická J, Schreiberová M, Viana M (2011). Reporting on ambient air quality assessment in the EU Member States, 2009. ETC/ACC Technical Paper 201/7. http://acm.eionet.europa.eu/reports/ETCACM_TP_2011_7_AQQ2009
JRC (2009). population density data 2009. Population density disaggregated with Corine land cover 2000. 100x100 m grid resolution, EEA version pop01clcv5.tif of 24 Sep 2009. http://www.eea.europa.eu/data-and-maps/data/population-density-disaggregated-with-corine-land-cover-2000-2
Malherbe L, Ung A, Colette A, Debry E (2012). Formulation and quantification of uncertainties in air quality mapping, ETC/ACM Technical Paper 2001/9. http://air-climate.eionet.europa.eu/reports/ETCACM_TP_2011_9_AQmapping_uncertainties
Mareckova K, Wankmüller R, Pazdernik K, Purzner M, Zechmeister A, Joebstl R, Adams M (2011). Inventory Review 2011. Review of emission data reported under the LRTAP Convention and NEC Directive. Stage 1 and 2 Review. Technical Report CEIP 1/2011. http://webdab1.umweltbundesamt.at/download/Reports/2011/InventoryReport2011_forWeb.pdf
Mol WJA, van Hooydonk PR, de Leeuw FAAM (2011). European exchange of monitoring information and state of the air quality in 2009. ETC/ACM Technical Paper 2011/1. http://air-climate.eionet.europa.eu/reports/ETCACM_TP_2011_1_EoI_AQ_meta_info2009
ORNL (2008). ORNL LandScan high resolution global population data set. http://www.ornl.gov/sci/landscan/landscan_documentation.shtml
Simpson D, Fagerli H, Jonson JE, Tsyro S, Wind P, Tuovinen J-P (2003). Transboundary acidification and eutrophication and ground level ozone in Europe: Unified EMEP model description. EMEP Status Report 1/03 Part I. MNP, Oslo, Norway. http://www.emep.int/publ/reports/2003/emep_report_1_part1_2003.pdf
Simpson D, Gauss M, Tsyro S., Valdebenito Á (2011). Chapter 8 Model Updates. In: Transboundary Acidification, Eutrophication and Ground Level Ozone in Europe in 2008, EMEP Report 1/2011. http://emep.int/publ/reports/2011/status_report_1_2011.pdf

UNECE (2004). Mapping Manual 2004. Manual on methodologies and criteria for Modelling and Mapping Critical Loads ands Levels and Air Pollution Effects, Risks and Trends. United Nations – Economic Commission for Europe, LRTAP Convention. http://www.oekodata.com/icpmapping/htm/manual/manual_eng.htm

UN (2010). World Population Prospects - The 2010 Revision, Highlights. United Nations. Department of Economic and Social Affairs, Population Division. New York. http://esa.un.org/unpd/wpp/index.htm